Technical Report

TR-13-27

Localised corrosion of copper canisters in bentonite pore water

Fraser King, Integrity Corrosion Consulting Limited

Christina Lilja, Svensk Kärnbränslehantering AB

December 2013

Svensk Kärnbränslehantering AB
Swedish Nuclear Fuel
and Waste Management Co

Box 250, SE-101 24 Stockholm
Phone +46 8 459 84 00

ISSN 1404-0344
SKB TR-13-27
ID 1419714

Localised corrosion of copper canisters in bentonite pore water

Fraser King, Integrity Corrosion Consulting Limited

Christina Lilja, Svensk Kärnbränslehantering AB

December 2013

Keywords: Pitting, Surface roughening, Active versus passive behaviour, Sulphate, Chloride, Bicarbonate, Pore-water composition, Probabilistic analysis.

Summary

The Swedish Radiation Safety Authority (SSM) has requested additional information on various aspects of SKB's license application for the disposal of spent nuclear fuel. As part of that request, SSM has asked for further information about the localised corrosion of copper canisters. This report describes additional analyses of the probability and nature of localised corrosion of the canisters based on a review of information in the literature and an assessment of the near-field environmental conditions to which the canisters will be exposed. No new experimental work has been performed.

The analysis has involved a number of steps. First, the nature of the environment at the canister surface and how it evolves with time have been reviewed and the time-dependent pore-water composition and canister surface temperature have been defined. Next, the available literature evidence on the localised corrosion of copper has been reviewed. Localised corrosion may take the form of discrete pitting or general surface roughening. As part of this review, the conditions under which the copper canister surface would be expected to be either passive or to dissolve actively have been reviewed. Finally, the expected canister surface environmental conditions have been compared to those that support pitting of copper from which the expected corrosion behaviour of the canister has been determined.

Based on the expected near-field environmental conditions, it is concluded that the canister will not be susceptible to discrete pitting corrosion but will instead undergo general corrosion under actively dissolving conditions. This conclusion is consistent with (i) the observations of surface roughening from large-scale *in situ* tests at the Äspö laboratory, (ii) the nature of copper surfaces following exposure to simulated repository conditions, (iii) the thermodynamic conditions under which copper is known to passivate, and (iv) the general lack of pitting data in the literature for the pore-water composition of the bentonite surrounding the canister.

Contents

1 Introduction

1.1 Background

The copper canister will be subject to a number of corrosion processes in the repository. Because of the nature of the environment to which the canister will be exposed and the corrosion properties of copper, the predominant process is expected to be general corrosion. Corrosion is not expected to be perfectly uniform, and there will likely be some degree of localised corrosion of the canister. Here the term "localised corrosion" is used to refer to any process that leads to the non-uniform corrosion of the surface, and could refer to minor surface roughening of an otherwise uniformly corroded surface or discrete pitting corrosion in the classical sense of the term and which is characterised by permanent spatial separation of the anodic and cathodic processes.

In SR-Site, the primary argument used to account for localised corrosion is that the canister will be subject to surface roughening, and not discrete pitting corrosion (SKB 2011, Section 12.6.2). This argument is based on observations from large-scale *in situ* tests (such as the Canister Retrieval Test (CRT), the Prototype Repository (Taxén et al. 2012) and Long-term test of buffer material (LOT) (Karnland et al. 2009)) and from the results of corrosion experiments conducted under simulated repository conditions (King et al. 2010). In both cases, the entire surface of the copper canister or corrosion coupon is observed to have been generally corroded, with deeper penetrations in some locations. Quantitatively, the extent of localised corrosion is accounted for in the canister lifetime predictions using a "surface roughening allowance" amounting to a few tens of micrometres (SKB 2010a, Section 3.5.4).

A secondary argument that has been used for the localised corrosion of copper canisters is the comparison of the corrosion potential (E_{CORR}) to the pitting or film-breakdown potential (E_b) (King 2002, King et al. 2010). Since the predicted E_{CORR} value is several hundred millivolts below the value of E_b, it was concluded that pits would not initiate on the canister surface, consistent with the available experimental evidence and the observations from full-scale tests mentioned above. Such an approach implicitly assumes that the surface of the copper is in a passive condition, rather than corroding actively, although there is no evidence to indicate that this is indeed the case. For this reason, the assessment of localised corrosion based on the comparison of the values of E_{CORR} and E_b has been used as a secondary argument for localised corrosion, in favour of the primary argument based on the surface roughening allowance.

The Swedish Radiation Safety Authority (SSM) has requested additional analyses of the localised corrosion of the copper canister (SSM 2012). The basis of the request for additional information is the treatment of pitting corrosion using the comparison of E_{CORR} and E_b. In particular, based in part on the review of Scully and Hicks (2012), SSM has requested that:

- SKB should perform a probabilistic assessment of the risk of pitting corrosion under both oxic and anoxic conditions.
- The assessment should (i) address how large a potential difference between E_{CORR} and E_b is necessary to demonstrate that pitting is of no concern; (ii) describe models for E_{CORR} and E_b as a function of ground water composition, radiolysis, and temperature; and (iii) account for the effects of salt enrichment before buffer saturation and salt deposits on the canister surface.

1.2 Methodology and structure of report

This report describes a series of analyses that have been performed to assess the likelihood of localised corrosion of the canister, and to address, as far has been possible, the specific requests of SSM described above. Figure 1-1 shows the overall approach used for a probabilistic analysis.

In order to assess the localised corrosion behaviour, it is necessary to first understand the nature of the environment *at the canister surface* and how that environment evolves with time. The near-surface environment is quite different from that in the bulk ground water, largely because of the presence and properties of the highly compacted bentonite, and for this reason the nature of the corrosive conditions is first described in some detail (Chapter 2).

The next step is then to describe the corrosion behaviour of the canister in these environmental conditions (Chapter 3) based on a review of the relevant technical literature, not only of the pitting of copper but also of the conditions under which the surface would be expected to be either passive (and, hence, subject to the possibility of pit initiation and growth) or active (and, hence, subject to general corrosion only). Particular attention is paid in this review to the effects of the important pore-water species, namely chloride (Cl^-), sulphate (SO_4^{2-}), bicarbonate (HCO_3^-), and sulphide (HS^-), as well as the pore-water pH, temperature, and redox potential (E_h). In addition, the general corrosion behaviour of copper in these environments is also briefly described, as this largely determines the value of E_{CORR} and how it would be modelled, as described in the SSM request.

The crucial next step is to determine whether, under the expected environmental conditions at the canister surface, the canister will be in a passive state and subject to pitting corrosion. This is done in Chapter 4, based on the relevant environmental and corrosion information from Chapter 2 and Chapter 3, respectively.

If the canister is likely to be in a "pitting condition" at some stage during its service life then a probabilistic assessment is performed of the pitting criterion (i.e., $E_{CORR} \geq E_b$), using appropriate probability distribution functions (pdf's) for the distributed parameters E_{CORR} and E_b. If pit initiation is possible, then the period of pit growth can be estimated from the length of time for which E_{CORR} exceeds the re-passivation potential, again taking into account the uncertainty and variability in these parameters. Finally, the extent of pit damage can be estimated by multiplying the pitting period by a suitable pit-growth rate law.

However, the available information indicates that the canister surface will be active under all repository conditions and will not be subject to pitting. For this reason, there are no available E_b data with which to carry out the probabilistic analysis. Nevertheless, the effects of pore-water composition, temperature, radiolysis, and surface deposits and salt enrichment are briefly discussed (see Section 4.2 to Section 4.4), as requested by SSM.

Chapter 5 presents the summary and conclusions.

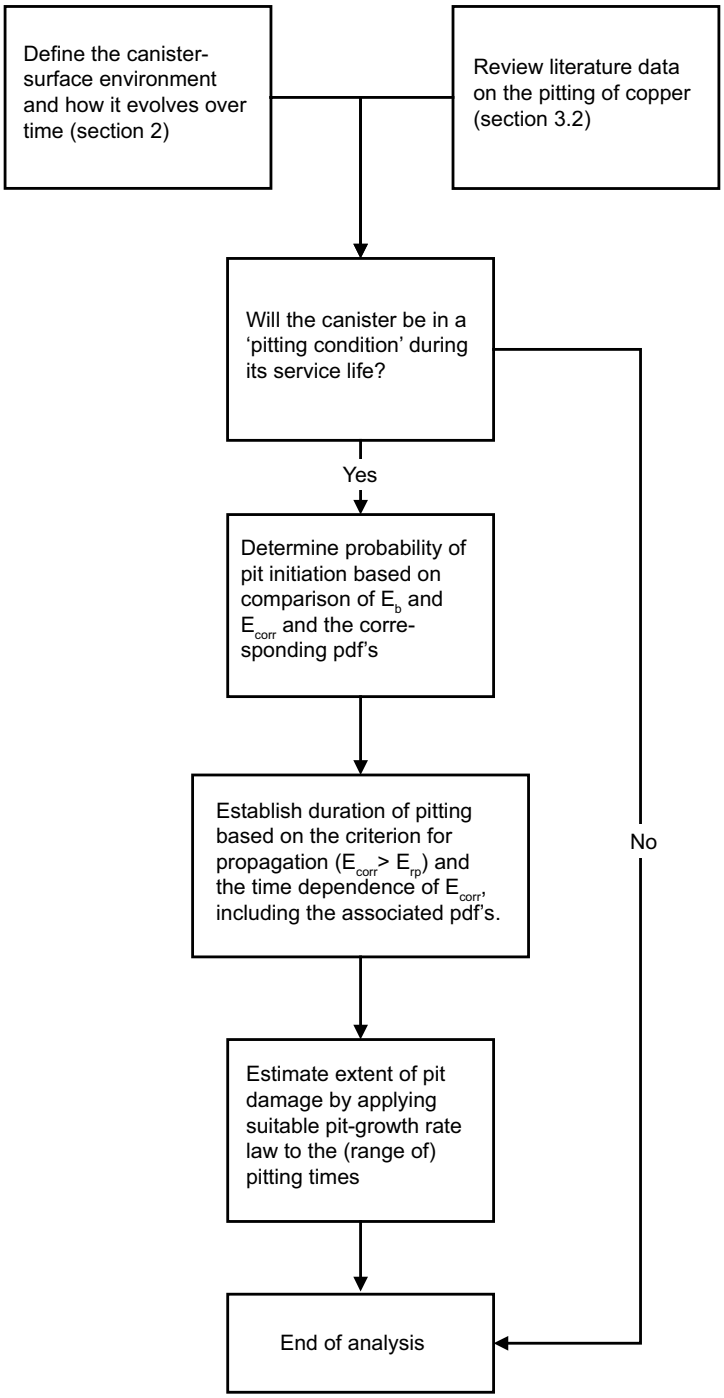

Figure 1-1. *Overall approach for addressing SSM question on probabilistic analysis of pitting of copper canisters.*

2 Evolution of the canister environment

2.1 General considerations

As noted above, the canister surface environment will differ from that in the ground water because of the presence of highly compacted bentonite and because of the thermal gradient resulting from the decay of the spent fuel. The bentonite will be emplaced with a degree of saturation of 60–70%, with the unsaturated fraction of the pore space filled with air. The initial pore-water composition will be determined by the composition of the water added to compact the clay (typically potable water) and the amounts of soluble mineral phases that will dissolve upon wetting of the dry clay prior to compaction. Depending upon the predominant exchangeable cation in the clay (Na^+ in the case of MX-80 bentonite and Ca^{2+} in the case of Deponit CA-N), ion exchange leads to an increase in pore-water Na^+ ion concentration in the case of MX-80 bentonite and Ca^{2+}/Mg^{2+} concentration in the case of Deponit CA-N. As the bentonite saturates with incoming ground water, the pore-water composition will equilibrate with the ground water. However, complete equilibration of the pore- and ground-water compositions may take a long period of time as, following saturation, transport of ions will primarily occur by diffusion.

In addition to these chemical and mass-transport processes, the composition of the pore water will also depend on the temporal and spatial changes in temperature. Salts and minerals with retrograde solubility (i.e., those for which the solubility decreases with increasing temperature) will tend to precipitate closer to the canister than those that exhibit an increase in solubility with increasing temperature. As the temperature decreases with time, previously soluble species may precipitate or, in the case of those with retrograde solubility, dissolve. Salt redistribution in bentonite pore water has been observed experimentally in both laboratory- (Cuevas et al. 1997) and large-scale (Dixon et al. 1998, Karnland et al. 2000) experiments. In some cases, pore water has been extracted by applying pressure to compacted bentonite samples, whereas in others the total salt content has been determined by leaching bentonite samples. In laboratory studies using a heated plate in contact with a compacted Spanish bentonite, Cuevas et al. (1997) observed an enhancement in Cl^- content of the pore water close to the heat source, but no corresponding enrichment in sulphate. Dixon et al. (1998) observed enrichment of both Cl^- and SO_4^{2-} close to the surface of a heater embedded in a compacted 50:50 sand:Canadian bentonite buffer mixture following a 900-day large-scale test. However, in the LOT experiment at the Äspö Hard Rock Laboratory, Karnland et al. (2000) observed only enrichment of sulphate close to the heated surfaces in contact with MX-80 bentonite. In contrast, the chloride concentration profile showed no enrichment at the heated Cu surface (Karnland et al. 2009). Svensson et al. (2011) also failed to observe any enrichment of Cl^- at the heater surface for a range of bentonite types in the alternative buffer material (ABM) test package 1 (Figure 2-1). Thus, there is no definitive answer to the question of whether salt enrichment occurs, and the effect needs to be considered in the following analysis.

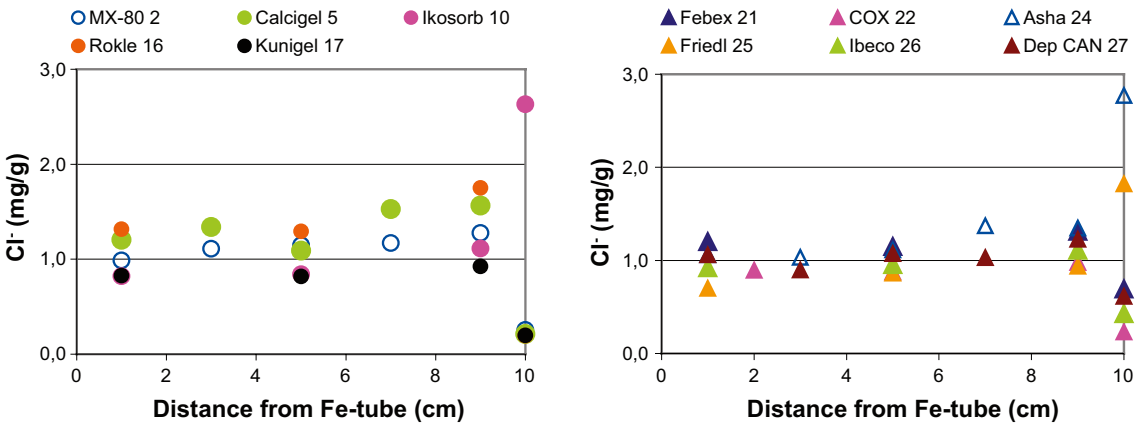

Figure 2-1. *The radial distribution of Cl^- in water extracts of the bentonite from the lower (left) and upper (right) part of the alternative buffer material (ABM) package 1 (Svensson et al. 2011). The reference samples (material analyses before the start of the experiment) are plotted at the position of 10 cm. The exposure time was more than 2 years. The type of bentonite and the position of the block in the package are indicated in the legend.*

At the same time, the redox conditions in the pore water will evolve. The trapped atmospheric O_2 will result in oxic conditions initially, with the establishment of anoxic conditions expected within a few months to a few tens of years (Muurinen 2006, Muurinen and Carlsson 2010, Puigdomenech et al. 2001, Olsson et al. 2013) as the residual oxygen is consumed by reaction with oxidisable impurities in the clay, by corrosion of the canister, and by aerobic microbial activity in regions outside of the compacted bentonite. Eventually, sulphide ions HS^- will diffuse from the ground water and contact the canister surface resulting in deeply anaerobic conditions, which are expected to persist indefinitely.

Thus, there will be an overall evolution of bentonite pore-water conditions from an early warm, aerobic phase to an eventual cool, anaerobic condition dominated by the presence of HS^-. Some of the shorter-term changes in pore-water chemistry have been studied experimentally (Cuevas et al. 1997, Karnland et al. 2009, Muurinen and Lehikoinen 1999), the results of which have been used to validate a number of numerical models developed to predict the evolution of pore-water conditions (Arcos et al. 2000, Bruno et al. 1999, Curti and Wersin 2002, Lemire and Garisto 1989, Luukkonen 2004, Nagra 2002, Sena et al. 2010a, b, Xie et al. 2006).

The evolution of the pore-water composition (and temperature) at the canister surface based on the results of numerical models is described in the following two sections for the oxic/early anoxic phase and for the long-term anoxic period.

2.2 Oxic and early anoxic period

For the oxic and early anoxic phases (i.e., prior to the ingress of HS^-), the modelling studies of Sena et al. (2010a) are used here to define the evolution of the canister-surface environment. Sena et al. (2010a) used the codes TOUGHREACT and PHAST to simulate the thermal and chemical evolution of the near field during the thermal transient and under saturated conditions, respectively. The predictions of the TOUGHREACT code for the thermal phase have been validated against measurements from the LOT experiment (Sena et al. 2010b). Simulations were performed for both MX-80 and Deponit CA-N bentonites, for different assumed saturation times (10, 100, or 1,000 years), and for high or low advective flow rates in the fracture assumed to intersect the borehole. The only complete data set presented by Sena et al. (2010a) (i.e., values for the interfacial $[Cl^-]$ and $[HCO_3^-]$, pH, and canister surface temperature) was for the case of MX-80 bentonite, 10-year saturation, and both high and low advective flows. Values for the interfacial concentrations and pH were taken directly from the corresponding profiles in Sena et al. (2010a). Pore-water sulphate concentrations have been estimated based on the solubility of the least-soluble calcium sulphate phase for the given temperature (Posnjak 1938).

As discussed in more detail in Chapter 3, the ionic species of interest for the localised (and general) corrosion of copper are Cl^-, SO_4^{2-}, and HCO_3^-, in addition to the pH of the pore water and the canister surface temperature. The ratios of the different anionic constituents can also indicate the relative tendencies to pitting or general corrosion. Tables 2-1(a) and 2-1(b) show the predicted time dependences for the canister surface temperature, and interfacial pH, $[HCO_3^-]$, and $[Cl^-]$ for the cases of high and low advective flow rates, respectively, extracted by the current authors from the figures provided by Sena et al. (2010a). The corresponding interfacial $[SO_4^{2-}]$ was calculated based on the solubility of calcium sulphate, with anhydrite ($CaSO_4$) being the least-soluble phase at temperatures >40°C and gypsum ($CaSO_4 \cdot 2H_2O$) being the least soluble form at lower temperatures (Posnjak 1938). Both calcium sulphate phases exhibit retrograde solubility at temperatures >40°C. Sena et al. (2010a) predict the precipitation of anhydrite during the thermal transient, which then progressively dissolves as the temperature decreases, being eventually replaced by precipitated gypsum.

In general, the pore water is predicted to be chloride-dominated with a near-neutral pH. For the simulations, the initial pore-water composition was assumed to be that measured in the LOT A2 experiment (Karnland et al. 2009, Sena et al. 2010b), which was used to validate the TOUGHREACT predictions. The $[Cl^-]$ gradually increases with time as the bentonite first saturates with incoming ground water (in the first 10 years) and then more slowly equilibrates with the ground water (Table 2-1(c)), with equilibration predicted to occur faster for the high advective fracture flow. In all cases, the pore-water $[HCO_3^-]$ is of the order of 10^{-3} mol/L, with $[SO_4^{2-}]$ in the range 0.01–0.02 mol/L, depending upon the temperature. The ionic concentration ratios shown in the table indicate that Cl^- is the predominant anion, with low $[HCO_3^-]$:$[Cl^-]$ and $[HCO_3^-]$:$[SO_4^{2-}]$ molar ratios.

Table 2-1. Predicted evolution of MX-80 bentonite pore-water chemistry at the canister surface (Sena et al. 2010a).

(a) 10-year bentonite saturation, high advective flow in fracture*

Time (years)	Temp. (°C)	pH	$[HCO_3^-]$ (mol/kg)	$[Cl^-]$ (mol/kg)	$[SO_4^{2-}]$ (mol/kg)	$[Cl^-]:[SO_4^{2-}]$	$[HCO_3^-]:[Cl^-]$	$[HCO_3^-]:[SO_4^{2-}]$
0	46	7.86	0.0011	0.040	0.0146	2.7	0.03	0.07
1	71	7.36	0.0011	0.040	0.0097	4.1	0.03	0.11
10	80	7.17	0.0014	0.072	0.0084	8.6	0.02	0.16
100	63	7.12	0.0016	0.094	0.0115	8.2	0.02	0.14
500	50	–	–	0.129	0.0137	9.4	–	–
1,000	41	6.96	0.0021	0.147	0.0156	9.4	0.01	0.13
10,000	20	7.07	0.0022	0.154	0.0149	10.3	0.01	0.15

(b) 10-year bentonite saturation, low advective flow in fracture*

Time (years)	Temp. (°C)	pH	$[HCO_3^-]$ (mol/kg)	$[Cl^-]$ (mol/kg)	$[SO_4^{2-}]$ (mol/kg)	$[Cl^-]:[SO_4^{2-}]$	$[HCO_3^-]:[Cl^-]$	$[HCO_3^-]:[SO_4^{2-}]$
0	46	7.86	0.0011	0.040	0.0146	2.7	0.03	0.07
1	71	7.36	0.0011	0.040	0.0097	4.1	0.03	0.11
5	79	–	–	0.062	0.0086	7.2	–	–
10	80	7.12	0.0013	0.072	0.0084	8.6	0.02	0.16
50	73	–	–	0.082	0.0095	8.6	–	–
100	63	7.05	0.0014	0.082	0.0115	7.1	0.02	0.12
1,000	41	7.12	0.0015	0.084	0.0156	5.4	0.02	0.09
10,000	20	7.27	0.0016	0.092	0.0149	6.2	0.02	0.10

(c) Forsmark ground water

Time (years)	Temp. (°C)	pH	$[HCO_3^-]$ (mol/L)	$[Cl^-]$ (mol/L)	$[SO_4^{2-}]$ (mol/L)	$[Cl^-]:[SO_4^{2-}]$	$[HCO_3^-]:[Cl^-]$	$[HCO_3^-]:[SO_4^{2-}]$
–	15	7.2	0.002	0.153	0.007	22.5	0.01	0.32

* The dash indicates that data for this time period were not available in Sena et al. (2010a).

Sena et al. (2010a) did not consider the evolution of redox conditions but simulations (Bruno et al. 1999, King and Kolář 2006, Wersin et al. 1994) and the results from large-scale tests (Muurinen 2006, Puigdomenech et al. 2001, Olsson et al. 2013) suggest that the time to establish anoxic conditions could range from a few months to a few tens of years. The longer time periods correspond to that required to consume not only the initially trapped atmospheric O_2 but also Cu(II) species formed from the oxidation of Cu(I) by O_2 (King and Kolář 2006).

2.3 Long-term anoxic period

King et al. (2011a, b) have developed a model, the CSM (Copper Sulphide Model), to predict the evolution of the repository environment from the initial oxic period through to the long-term anoxic phase in which the redox conditions are dominated by the presence of HS^-. Unlike the TOUGHREACT simulations of Sena et al. (2010a, b), the CSM does not take into account the various processes that determine the pore water concentrations of HCO_3^- and SO_4^{2-}, such as the buffering by calcite or the precipitation of calcium sulphate phases, but it does incorporate a number of processes for the formation and transport of HS^-. The results of the CSM model are used here to predict the time-dependent HS^- concentration at the canister surface.

Table 2-2 lists the predicted interfacial concentration of HS^- during the long-term anoxic period for a CSM simulation of the evolution of the repository based on the conditions at the Forsmark site (King et al. 2011b). Details of the input and other model parameters are provided by King et al. (2011a, b). In this simulation, the interfacial $[HS^-]$ is predicted to be higher than that in the ground water (1×10^{-5} mol/L, 0.3 mg/L) because sulphide is assumed to be produced in the bentonite by the dissolution of pyrite FeS_2 and in the adjacent backfill material by the microbial reduction of

Table 2-2. Predicted evolution of the interfacial sulphide concentration (King et al. 2011b). These data are taken from an unpublished output data file for the simulation referred to in the original reference.

Time (years)*	Temp. (°C)	$[HS^-]$ (mol/L)
1,185	40	8.5×10^{-6}
1,896	32	1.4×10^{-5}
3,034	26	1.9×10^{-5}
4,856	22	2.5×10^{-5}
12,420	17	3.5×10^{-5}
31,820	13	4.8×10^{-5}
81,680	11	5.9×10^{-5}
333,950	11	6.1×10^{-5}
539,300	11	6.2×10^{-5}
1,010,000	11	6.2×10^{-5}

* These times correspond to the output times from the CSM code which are determined by an arithmetic progression and, therefore, do not correspond to round numbers of years.

SO_4^{2-}, limited only by the availability of sulphate, the latter being in plentiful supply from both the ground water and the dissolution of sulphate minerals in the buffer and backfill materials. In fact, the rate of microbial sulphate reduction is expected to be limited by the availability of energy sources and organic carbon, so the results of this CSM simulation represent a worst case analysis. For this simulation, the ground water is a minor contributor to the accumulation of HS^- at the canister surface so that higher ground water $[HS^-]$ would not likely result in a higher interfacial concentration.

3 Corrosion behaviour of copper

3.1 Localised corrosion of copper canisters

As noted in Section 1.1, the primary evidence used to account for localised corrosion of the canisters in SR-Site is based on observations from long-term *in situ* tests and the results of laboratory corrosion experiments performed under simulated repository conditions (SKB 2010a, 2011). Figure 3-1 shows the surface profile of a copper coupon exposed to compacted 50:50 bentonite:sand buffer material saturated with initially aerated synthetic ground water solution and exposed at a temperature of 50°C for a period of 2 years (King et al. 2010, Litke et al. 1992). This surface profile is not consistent with a classical pitting mechanism in which anodic and cathodic reactions are spatially separated since the entire surface has corroded, albeit with slightly greater penetration in some areas than others (note the difference in vertical and horizontal scales in the figure). Instead, this profile is consistent with a mechanism in which the surface is primarily undergoing active dissolution, although there must either be faster corrosion in some locations or some temporary spatial separation of anodic and cathodic processes to account for the locally deeper penetrations. Although similar detailed surface profiles have not been measured, visual inspection of coupons from the LOT experiment (Karnland et al. 2000) and the Prototype (Rosborg 2013), as well as post-test electrochemical studies with samples from LOT (Rosborg and Werme 2008) also indicate the absence of pitting but the possibility of some uneven general corrosion. King et al. (2010) use the term "surface roughening" to describe this form of localised corrosion.

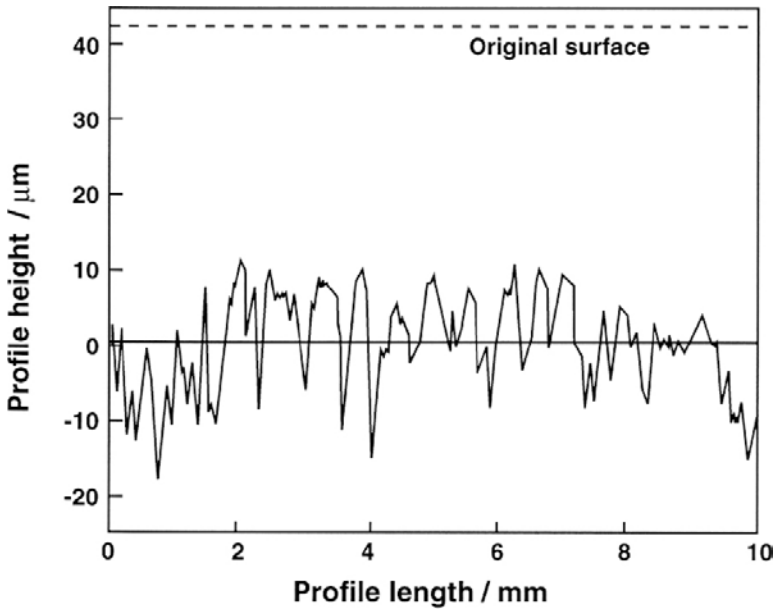

Figure 3-1. *Typical surface profile of stripped copper coupon following exposure to groundwater-saturated compacted buffer material at 50°C for 733 d (Litke et al. 1992).*

3.2 Pitting of copper

As noted in the Introduction and in the SSM request for additional information (SSM 2012), an alternative method for assessing the possibility of localised corrosion is the comparison of E_{CORR} and the breakdown (pitting) potential E_b. The criterion for the initiation of stable pits is that E_{CORR} is equal to or greater than E_b, i.e.,

$$E_{CORR} \geq E_b \quad (3\text{-}1)$$

Once initiated, a pit may continue to propagate until such time that the E_{CORR} drops below a so-called re-passivation potential E_{rp}. The extent of damage can then be estimated by multiplying the period of pit propagation by some suitable pit-growth expression. Scully and Hicks (2012) have proposed a methodology for assessing the probability of pit initiation, as well as the effects of pit stifling and re-passivation on canister penetration. Here, the discussion is limited to various aspects of pit initiation.

3.2.1 Effect of solution composition

The chemical species present in natural waters that most influence the pitting of copper are HCO_3^-, Cl^-, and SO_4^{2-}, and the pH. Increasing $[HCO_3^-]$ and pH tend to support passivation of copper, whereas Cl^- and SO_4^{2-} typically promote breakdown of surface films that can result in pit initiation (and growth). High HCO_3^- concentrations and/or pH can create a very passive surface that is immune to pit initiation. On the other hand, high $[Cl^-]$ and $[SO_4^{2-}]$ can cause such extensive film breakdown that the surface undergoes active dissolution rather than pitting. Thus, the occurrence of pitting requires a balance between factors that promote passivation and factors that lead to film breakdown.

Pitting of copper is a well-known issue in a range of potable waters in various countries. The early work of Pourbaix established that pitting occurred if the potential of the copper pipes exceeded a critical potential (Pourbaix 1969) which, in the widely studied Brussels tap water, has a value of approximately 0.10–0.17 V_{SCE}. Pitting also occurs in more saline environments (Drogowska et al. 1992, Gad Allah et al. 1991, Imai et al. 1996, Nishikata et al. 1990, Sridhar and Cragnolino 1993, Thomas and Tiller 1972a, b), although typically at higher pH than in potable waters.

In common with a range of passive alloys, Cl^- ions cause the local film breakdown and pitting of copper. Figure 3-2 shows the dependence of E_b on pH for a range of $[Cl^-]$ (as noted in the legend) in chloride-rich solutions, although in some cases the solution also contains HCO_3^- (and, in one case, SO_4^{2-}). The breakdown potential is typically determined from potentiodynamic scans, with the onset of film breakdown characterised by a rapid increase in current at a particular potential and positive hysteresis on the reverse potential scan (i.e., the current is higher during the reverse scan at a given potential than on the forward scan), generally confirmed by visually checking for pits on the electrode surface at the end of the experiment. In some studies, however, only the forward part of the scan is shown (or is even measured), whilst in others the extent of current hysteresis is limited. This makes it difficult in some cases to be certain that the authors did actually observe film breakdown, a difficulty that is compounded in the case of Cl^- by the fact that the current increases exponentially as the surface starts to actively dissolve. Therefore, it is possible that some of the reported E_b values are simply the potential at which active dissolution is observed, and this may explain the relatively negative E_b values reported by Drogowska et al. (1992).

Much of the observed variability in the E_b data in Figure 3-2 is the result of variation in the $[Cl^-]$ between the different studies. Despite this variability, it is apparent from the data that E_b increases with increasing pH. Of more interest here is that pitting only occurs at potentials more-positive than that for the formation of a Cu_2O or $Cu(OH)_2$ film, i.e., a certain degree of passivity is required for pitting.

A number of authors have highlighted the role of SO_4^{2-} in the pitting of copper (Christy et al. 2004, Cong 2009, Cong et al. 2009a, b, Duthil et al. 1996, Edwards et al. 1994, Imai et al. 1996, Mankowski et al. 1997, Mattsson and Fredriksson 1968, Milošev et al. 1992, Sridhar and Cragnolino 1993). Figure 3-3 shows a compilation of E_b values as a function of pH in sulphate-rich solutions. The data in sulphate solutions show a similar trend to those in Cl^- solutions, with the majority of E_b values above the equilibrium line for the $Cu_2O/Cu(OH)_2$ couple. In potable water, sulphate may be more aggressive than Cl^- (Edwards et al. 1994, Mattsson and Fredriksson 1968, Sridhar and Cragnolino 1993), although in more-saline solutions Cl^- appears to result in lower breakdown potentials than SO_4^{2-} at the same concentration (Figure 3-4 and Figure 3-5).

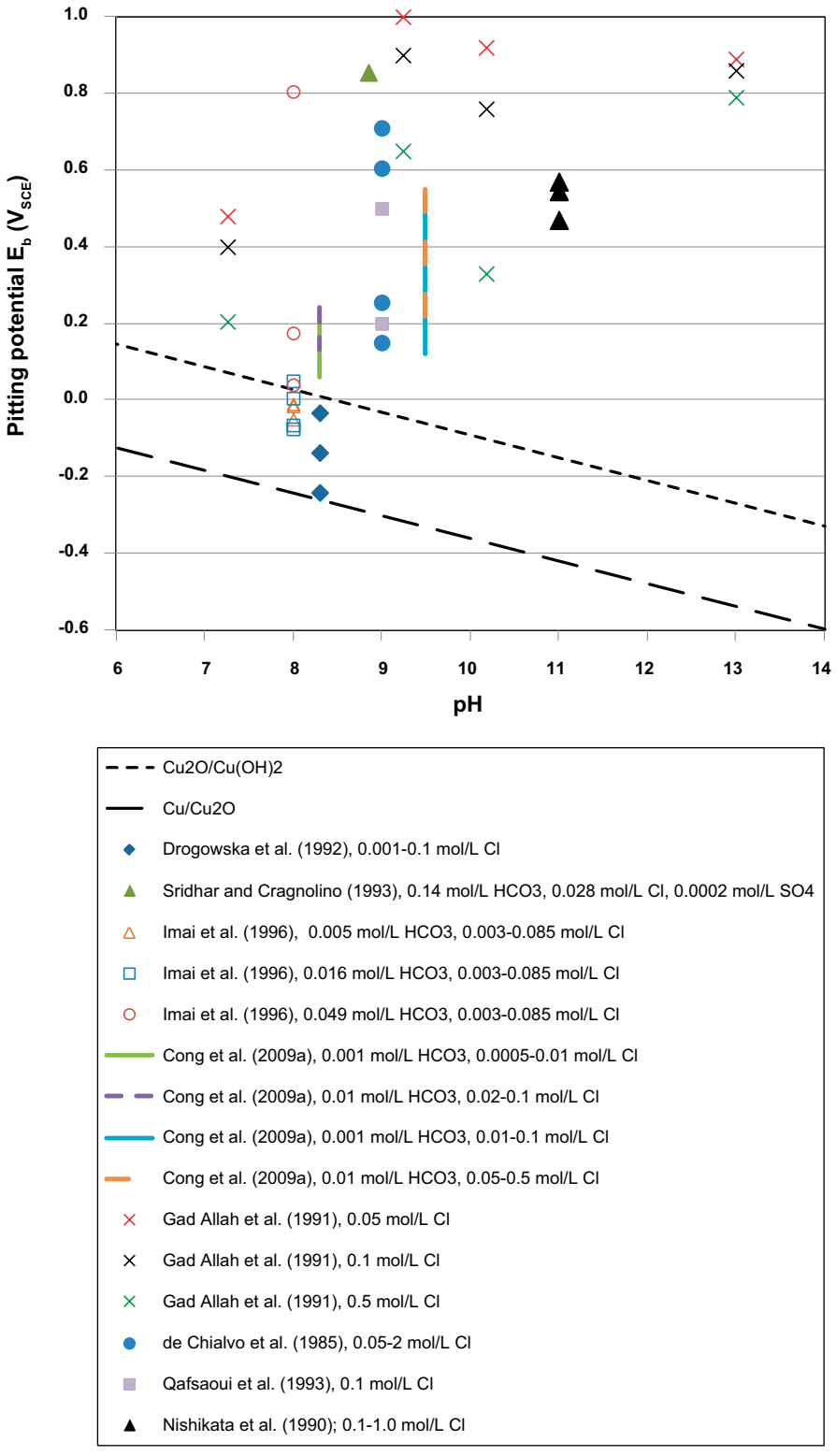

Figure 3-2. *Compilation of breakdown potentials for copper in chloride-rich solutions at temperatures of 23–30°C as a function of pH.*

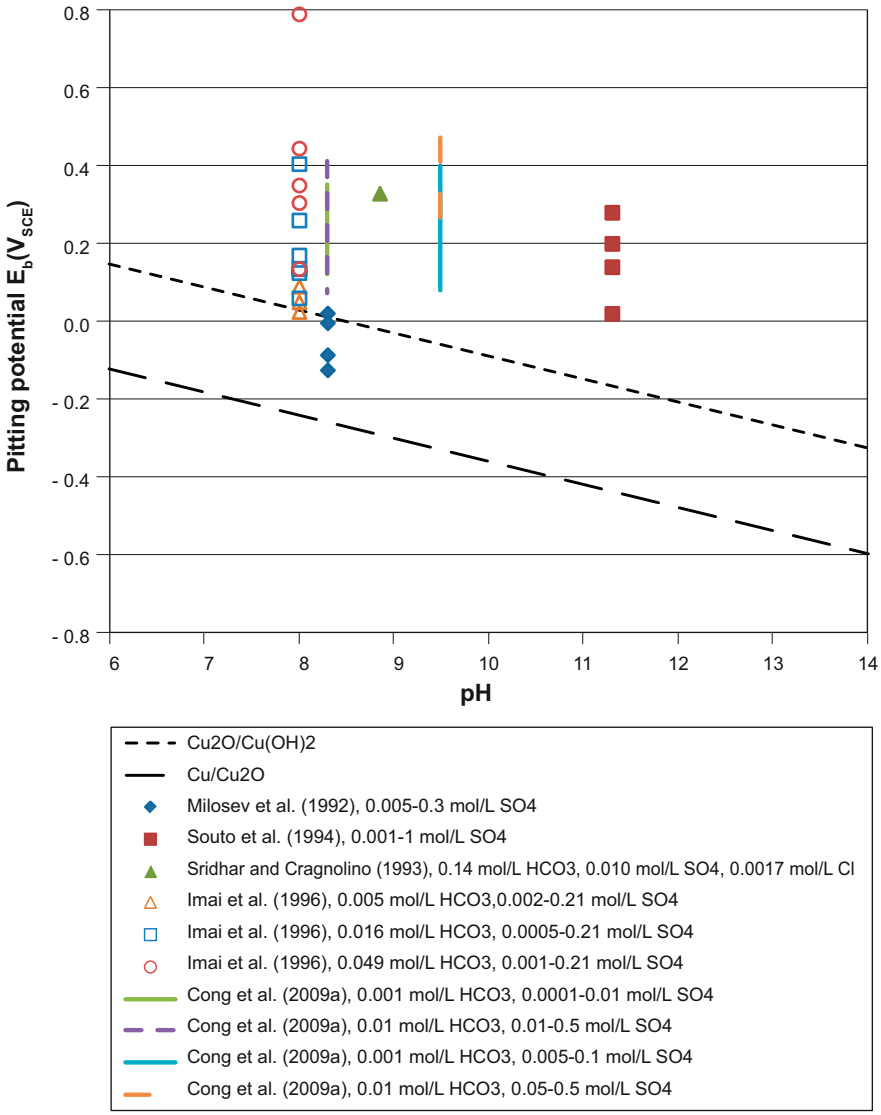

Figure 3-3. *Compilation of breakdown potentials for copper in sulphate-rich solutions at temperatures of 23–30°C as a function of pH.*

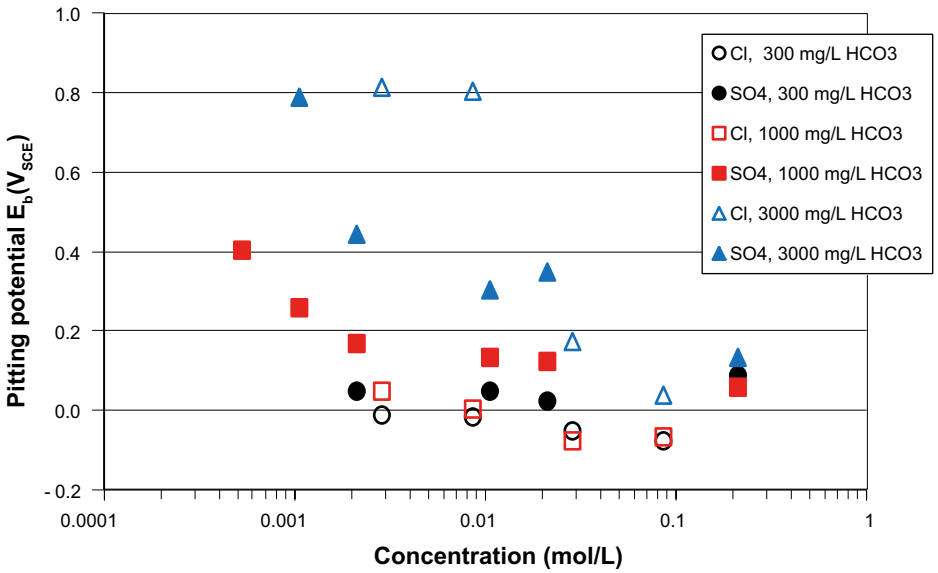

Figure 3-4. *Comparison of breakdown potentials for copper in sulphate- and chloride-containing bicarbonate solutions (Imai et al. 1996).*

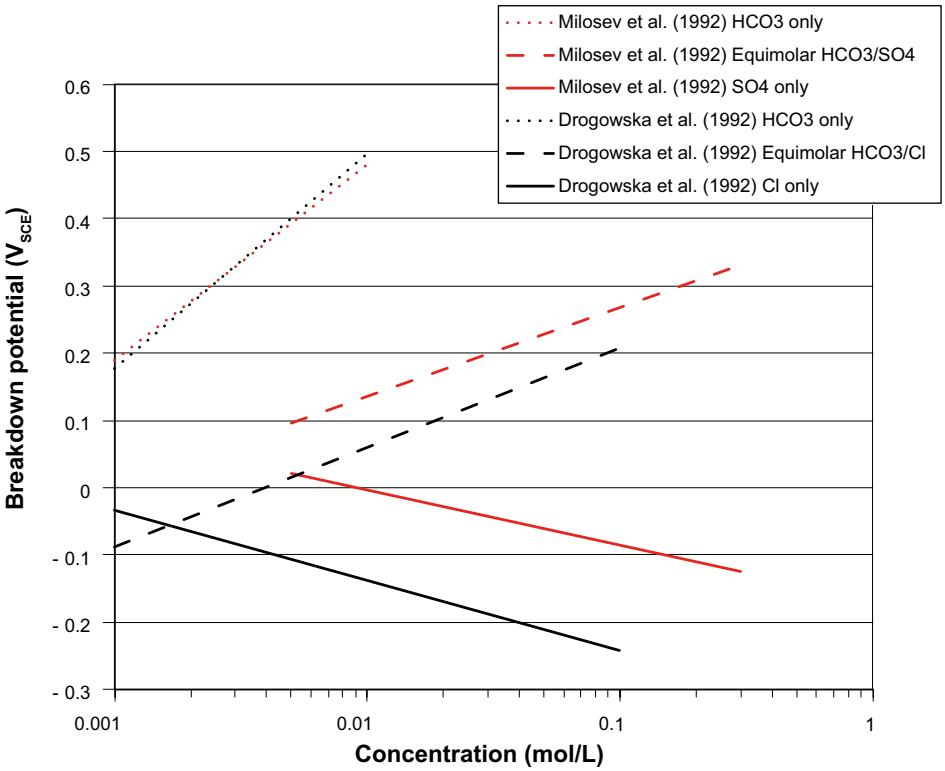

Figure 3-5. *Comparison of breakdown potentials for copper in bicarbonate, sulphate, chloride and in equimolar SO_4^{2-}/HCO_3^- and Cl^-/HCO_3^- solutions (Drogowska et al. 1992, Milošev et al. 1992).*

Duthil et al. (1996) and Mankowski et al. (1997) have suggested a synergistic effect between Cl^- and SO_4^{2-} on the pitting of copper. In mixed Cl^-/SO_4^{2-} solutions (0.01–0.05 mol/L SO_4^{2-}), three regions of behaviour are observed depending upon the Cl^- concentration. Based on the pit initiation rate, at low $[Cl^-]$ (≤ 0.0005 mol/L), SO_4^{2-} is responsible for pitting, with Cl^- also contributing to film breakdown with increasing concentration. At higher $[Cl^-]$ and for $[Cl^-]:[SO_4^{2-}]$ ratios ≤ 5, SO_4^{2-} is responsible for pitting, with Cl^- having an increasing inhibitive effect on film breakdown with increasing concentration, believed to be due to the formation of a protective CuCl layer (Mankowski et al. 1997). Finally, at $[Cl^-]:[SO_4^{2-}] > 5$, i.e., at $[Cl^-] > 0.05$–0.25 mol/L, Cl^- is predominantly responsible for pitting.

Bicarbonate ions play an important role in the pitting of copper. At low concentrations (less than approximately 100–300 mg/L (0.0016–0.005 mol/L), and at near-neutral pH, the copper surface is active and pitting is not observed (Imai et al. 1996, Sridhar and Cragnolino 1993). With increasing HCO_3^- concentration, the surface passivates and is susceptible to pitting (Sridhar and Cragnolino 1993). Bicarbonate ions also inhibit film breakdown, with E_b shifting to more-positive values with increasing HCO_3^- concentration (Figure 3-4 and Figure 3-5). Interestingly, the inhibitive effect of HCO_3^- is greater than the effect of either Cl^- or SO_4^{2-} on film breakdown, as indicated by the fact that E_b shifts to more-positive values with increasing concentration in equimolar mixtures of either Cl^- and HCO_3^- (Drogowska et al. 1992) or SO_4^{2-} and HCO_3^- (Milošev et al. 1992) (Figure 3-5).

In potable water, the effects of HCO_3^-, Cl^-, SO_4^{2-}, and OH^- on both the pitting and re-passivation potentials have been fitted to simple expressions, of the form (Cong 2009, Cong et al. 2009a, b)

$$E_b,\ E_{rp} = a + b\cdot\log[OH^-] + c\cdot\log[HCO_3^-] + d\cdot\log[SO_4^{2-},\ Cl^-] \qquad (3\text{-}2)$$

where a, b, c, and d are fitting parameters. For HCO_3^-/SO_4^{2-} solutions, the relationships for E_b and E_{rp} are, respectively

$$E_b = 1.11 + 0.116\cdot\log[OH^-] + 0.197\cdot\log[HCO_3^-] - 0.130\cdot\log[SO_4^{2-}]\ V_{SCE} \qquad (3\text{-}3)$$

and

$$E_{rp} = 0.073 + 0.0044\cdot\log[OH^-] + 0.0782\cdot\log[HCO_3^-] - 0.0593\cdot\log[SO_4^{2-}]\ V_{SCE} \qquad (3\text{-}4)$$

For HCO_3^-/Cl^- solutions, the relationships for E_b and E_{rp} are, respectively

$$E_b = 1.56 + 0.206 \cdot \log[OH^-] + 0.191 \cdot \log[HCO_3^-] - 0.123 \cdot \log[Cl^-]\ V_{SCE} \quad (3\text{-}5)$$

and

$$E_{rp} = -0.0925 + 0.00373 \cdot \log[OH^-] - 0.0139 \cdot \log[HCO_3^-] - 0.0566 \cdot \log[Cl^-]\ V_{SCE} \quad (3\text{-}6)$$

The similarity of the dependence of E_b on the sulphate and chloride concentrations lead Cong et al. (2009a, b) to suggest the following overall expression for the breakdown potential

$$E_b = 1.11 + 0.116 \cdot \log[OH^-] + 0.197 \cdot \log[HCO_3^-] - 0.130 \cdot \log([SO_4^{2-}] + [Cl^-])\ V_{SCE} \quad (3\text{-}7)$$

These expressions were developed from measurements at pH 8.3 and pH 9.5 and anion concentrations from approximately 10^{-4} mol/L to 0.5 mol/L, although the authors caution that the applicability of these expressions outside of the range of measurements is uncertain.

Pitting of copper has also been reported in concentrated sulphide solutions (Gennero de Chialvo and Arvia 1985, Vasquez Moll et al. 1985). In 0.001–0.05 mol/L Na_2S solutions at pH 9 and pH 14, Gennero de Chialvo and Arvia (1985) report pitting at potentials more positive than −0.54 V_{SCE}. Vasquez Moll et al. (1985) report a breakdown potential of −0.74 V_{SCE} in 0.01 mol/L Na_2S at pH 13. The relevance of breakdown potentials measured at such high $[HS^-]$ and at such high pH to the environments expected in the repository is unclear. Recently, Chen et al. (2010, 2011a, b, 2012) have shown that the properties of the film formed on copper in sulphide depend on both the $[Cl^-]$:$[HS^-]$ ratio and, more importantly, the flux of HS^- to the copper surface. Three types of behaviour have been observed. For the $[HS^-]$ and $[Cl^-]$ expected in the repository, films are porous and grow linearly with time due to slow HS^- transport. Such films are not passive and there is no evidence for localised corrosion of the surface. At higher $[HS^-]$ (≥ 0.001 mol/L), compact films can form, although even for these protective films no evidence for pitting has been observed. Thus, although King (2002) suggested that the canister might be subject to localised corrosion based on the limited information available at that time, the more recent information suggests that pitting will not occur due to the presence of HS^- under repository conditions.

The measured breakdown and re-passivation potentials are known to be distributed parameters, both because of the stochastic nature of the pitting process and because of variability inherent in the measurements. There are only a limited number of reports of the variability of E_b and E_{rp} for copper in the literature and no discussion of the shape of the distributions. Cong et al. (2009a, b) showed a plot of the cumulative distribution of E_b and E_{rp} values for copper exposed to a synthetic potable water at pH 9. Figure 3-6 shows the distributions for E_b and E_{rp} based on the experimental data given by Cong et al. (2009a, b).

Based on the data of Cong et al. (2009a, b), the mean breakdown potential for a synthetic potable water at pH 9.5 is 0.317 V_{SCE} with a standard deviation of 0.061 V. The mean re-passivation is 0.091 V_{SCE} with a standard deviation of 0.005 V. It is interesting to note that the spread in the E_b values is significantly larger than that in the re-passivation potential. Drogowska et al. (1992) report a standard deviation for E_b (the type of distribution was not defined) of 0.027 V in HCO_3^- solution and 0.042 V in Cl^- and HCO_3^-/Cl^- solutions. Gonzalez et al. (1993) report a ± value of 0.05 V for the breakdown potential of copper in 1 mol/L $NaClO_4$ solution and a smaller ± value of 0.01 V for the corresponding E_{rp}.

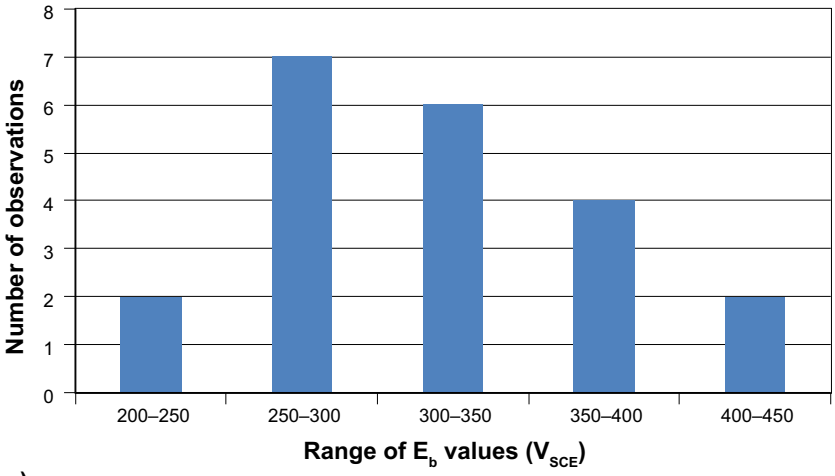

a)

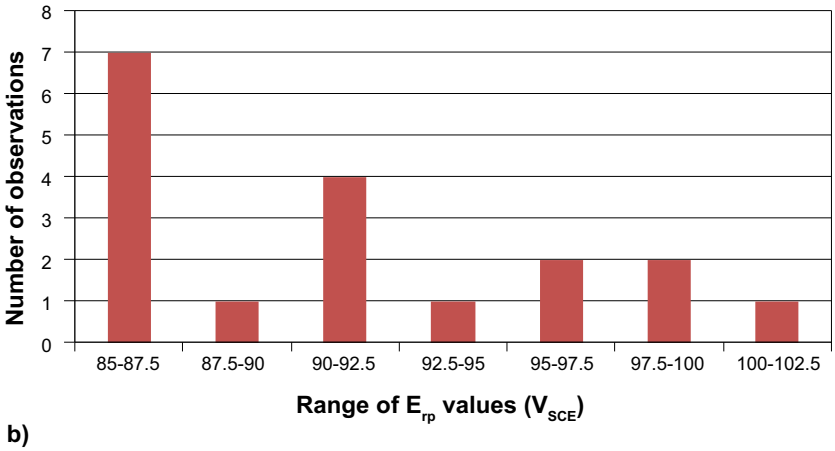

b)

Figure 3-6. *Distribution of measured* ***a) pitting (E_b)*** *and* ***b) re-passivation (E_{rp})*** *potentials for copper exposed to a synthetic potable water at pH 9.5 based on the data of Cong et al. (2009a, b).*

3.2.2 Effect of temperature

A number of authors have investigated the effect of temperature on the breakdown potential of copper. In general, above an apparent minimum at a temperature of approximately 15°C (Figueroa et al. 1986), E_b tends to increase with temperature, the one exception being the measurements of Thomas and Tiller (1972b) in a HCO_3^-/Cl^- mixture (Figure 3-7). The surface film apparently becomes more protective with increasing temperature and it is interesting to note that neither Skrypnikova et al. (2008) (at 70°C and 80°C) nor Sridhar and Cragnolino (1993) (at 95°C) observed pitting at elevated temperatures, whereas pitting was observed in the same environments at lower temperatures.

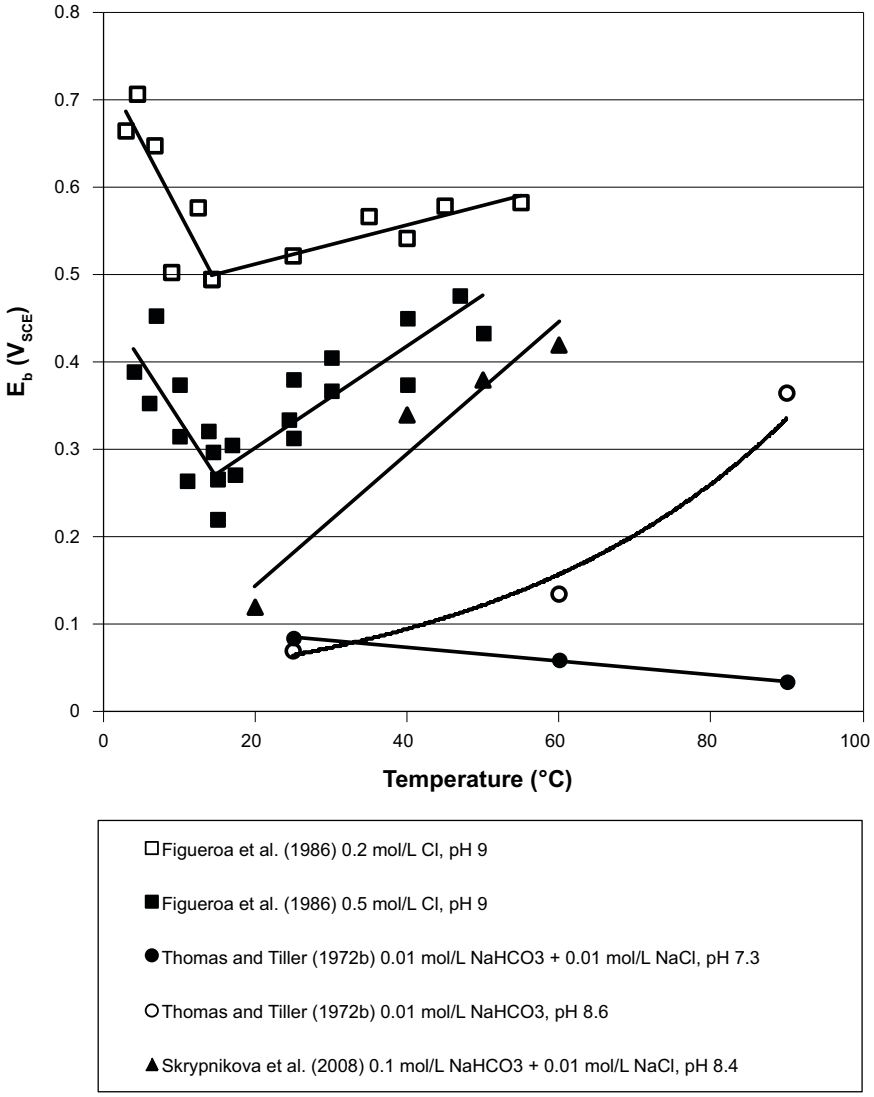

Figure 3-7. *Compilation of studies of the temperature dependence of the breakdown potential of copper in chloride and chloride/bicarbonate solutions.*

3.2.3 Effect of radiolysis

Pitting and re-passivation potentials of copper have not been measured in the presence of γ-radiation. Imai et al. (1996) measured E_b in Cl^-/HCO_3^- solutions as a function of dissolved O_2 concentration. Figure 3-8 shows the dependence of E_b on $[Cl^-]$ for solutions containing 300, 1,000, or 3,000 mg/L HCO_3^- under essentially deaerated conditions (dissolved $[O_2] < 0.5$ mg/L, open symbols) and under oxidising conditions (dissolved $[O_2] > 15$ mg/L, closed symbols). In general, the value of E_b is more positive at the higher dissolved $[O_2]$, especially at low $[Cl^-]$ and/or high $[HCO_3^-]$. Imai et al. (1996) also report a greater tendency towards passive behaviour in HCO_3^- solution with increasing $[O_2]$, indicating that the presence of O_2 in solution helps promote passive behaviour. It is not known whether this behaviour extends to other oxidants, such as those produced by γ-radiolysis.

As with all other factors, the effect of γ-radiation on the pitting of copper depends on the effects on both E_b and E_{CORR} and the consequent difference in potential. This effect will be considered in Section 4.3.

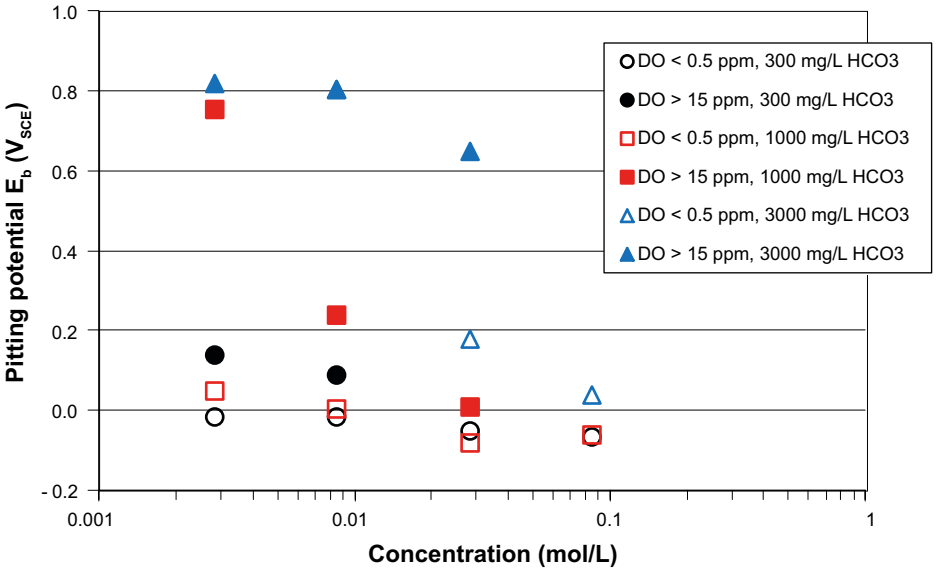

Figure 3-8. *Effect of dissolved oxygen on the breakdown potential of copper in chloride/bicarbonate solutions at neutral pH (Imai et al. 1996).*

3.2.4 Effect of surface deposits

Cong and Scully (2013) and Cong et al. (2007) have discussed the effects of $Al(OH)_3$ on the pitting of copper in potable waters. The addition of $Al(OH)_3$ to synthetic potable waters resulted in a decrease in E_b to potentials close to the re-passivation potential. Inert membranes had no effect. It is postulated that, in addition to acting as a physical membrane that can occlude surface sites, $Al(OH)_3$ sorbs anions (such as OH^-, Cl^-, SO_4^{2-}, and HCO_3^-) and thus creates a more acidic environment beneath the deposit. Preferential adsorption of OH^- would also lead to an increase in $[SO_4^{2-}]$:$[OH^-]$ ratio, which could enhance the probability of pitting (Cong and Scully 2013).

3.3 Conditions for active versus passive behaviour

It is evident from the discussion above that copper will only undergo pitting if the surface is passive. The passive film on copper consists of a duplex layer of Cu_2O and either CuO or $Cu(OH)_2$, with the outer Cu(II) layer primarily responsible for passivity (King 2002, King et al. 2010). The requirement for a Cu_2O/Cu(II) passive layer for pitting is highlighted by the distribution of E_b values in Cl^- (Figure 3-2) and SO_4^{2-} (Figure 3-3) solutions, all of which lie above the $Cu_2O/Cu(OH)_2$ equilibrium line, with the exception of those E_b values possibly mistaken for the potential at which active dissolution occurs (Drogowska et al. 1992, Milošev et al. 1992). In potable waters, Cong et al. (2009a) have shown a correspondence not only between E_b and the $Cu_2O/Cu(OH)_2$ equilibrium line but also between the transition between pitting and general corrosion at the pH corresponding to the value at which E_b is equal to the equilibrium potential for the $Cu_2O/Cu(OH)_2$ couple (Figure 3-9). In Cl^- environments, the range of pH and potential over which Cu_2O and CuO are thermodynamically stable is smaller because of the formation of $CuCl_2^-$ and $CuCl_2 \cdot 3Cu(OH)_2$ (Figure 3-10).

A number of authors have attempted to define the conditions under which copper exhibits either active (i.e., general as opposed to localised corrosion) or passive behaviour (Imai et al. 1996, Yabuki and Murakami 2007). Of primary concern here is whether, under freely corroding conditions, the surface dissolves actively or is subject to pitting. Yabuki and Murakami (2007) measured the frequency of pits and the rate of general corrosion of copper in Cl^- and SO_4^{2-} solutions as a function of concentration in unbuffered solutions at 60°C under freely corroding conditions. A transition was observed between general corrosion and pitting at a concentration of ~0.034 mol/L under static conditions (lower concentration threshold under flowing conditions). There was no difference in the threshold concentration in deaerated and O_2-containing solutions.

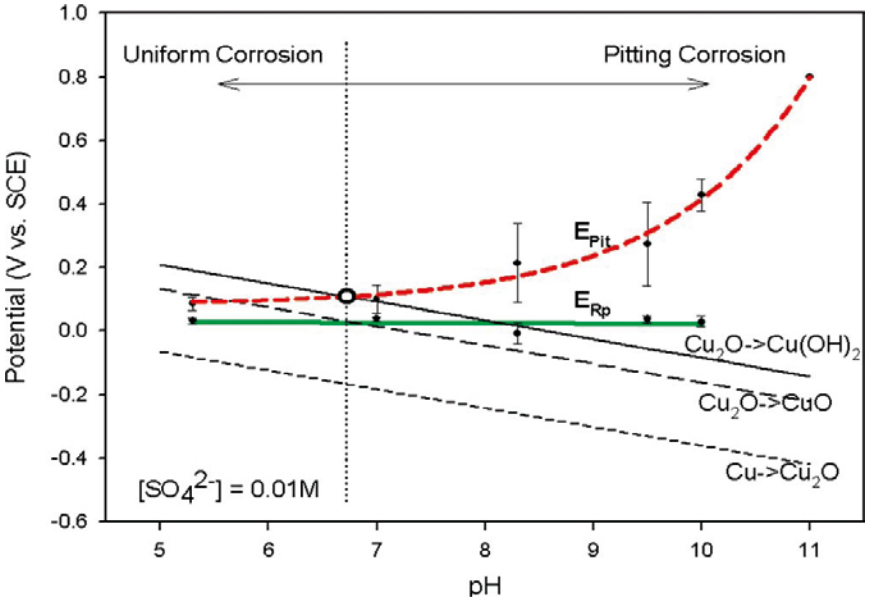

Figure 3-9. *Relationship between the breakdown and re-passivation potentials and the conditions for pitting and general corrosion and the thermodynamic stability of cuprous and cupric oxide/hydroxide films (Cong et al. 2009a).*

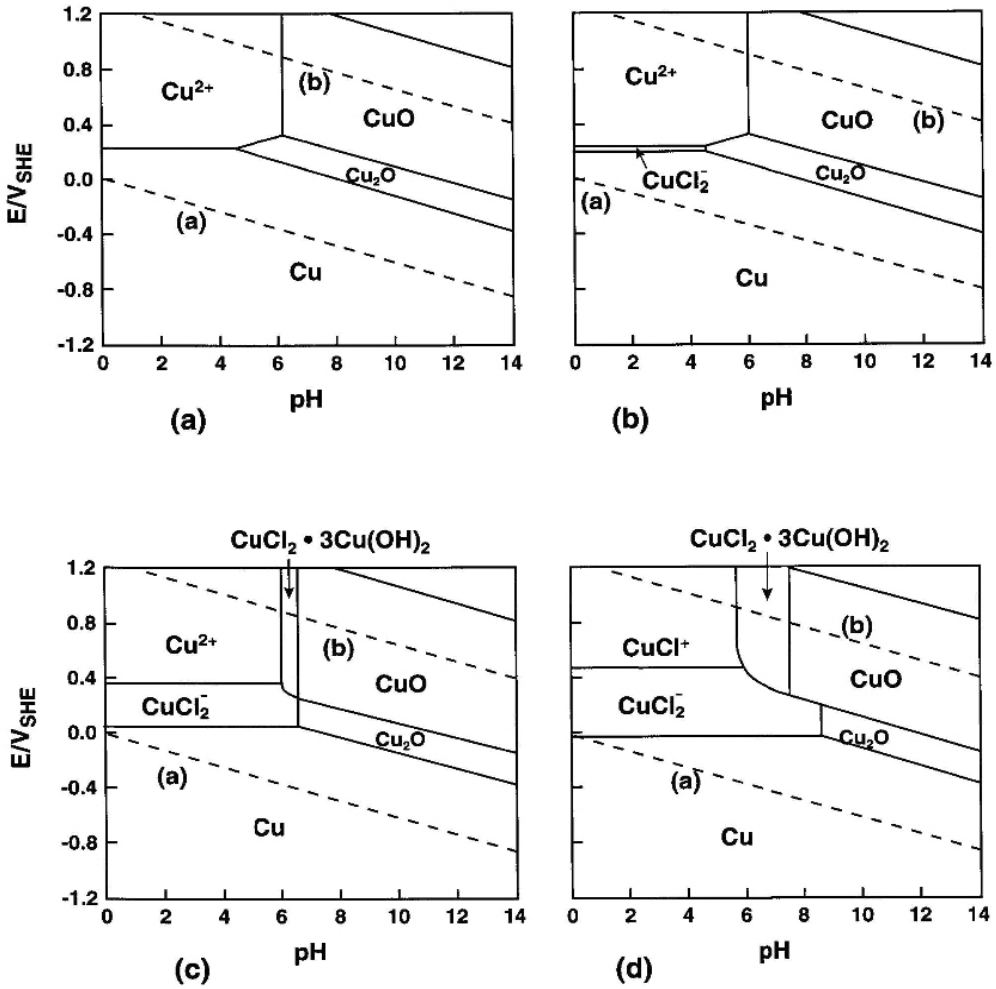

Figure 3-10. *Potential/pH (Pourbaix) diagrams for the system Cu/Cl⁻/H_2O at 25°C for various chloride concentrations. (a) 10^{-3} mol/L, (b) 10^{-2} mol/L, (c) 0.1 mol/L, (d) 1.0 mol/L. Figures constructed for a total dissolved Cu activity of 10^{-6} mol/L (King et al. 2010).*

Imai et al. (1996) characterised the active/passive behaviour of copper in HCO_3^- solutions containing either Cl^- or SO_4^{2-} as a function of dissolved O_2 concentration based on the characteristics of the measured current-potential behaviour (Figure 3-11). Experiments were conducted at 30°C at the natural pH of the solution, which was not defined but which is likely to be in the range pH 8–9. Active behaviour was promoted by increasing [Cl^-] and decreasing [HCO_3^-] and/or decreasing [O_2]. Similar behaviour was observed in SO_4^{2-}/HCO_3^- solutions.

Increasing [HCO_3^-], in particular, promotes passive behaviour (Figure 3-11, Imai et al. 1996). Sridhar and Cragnolino (1993) also report a transition from active behaviour at low [HCO_3^-] (85 mg/L, 0.0014 mol/L, pH 8–9) to passive behaviour at high [HCO_3^-] (8,500 mg/L, 0.14 mol/L, pH 8–9).

It is apparent, therefore, that elevated Cl^- and/or SO_4^{2-} concentrations, as might result from the redistribution of salts under the impact of the thermal gradient (Section 2.1), will tend to promote active dissolution rather than passivity.

3.4 General corrosion and the factors determining E_{CORR}

The corrosion potential E_{CORR} is the potential at which the sum of the rates of the anodic (oxidation) reactions equals the sum of the rates of the cathodic (reduction) reactions. In the case of the general corrosion of the surface, the anodic and cathodic surface areas are equal and are equal to the geometric surface area.

In O_2-containing Cl^- solutions, the mechanisms of the anodic and cathodic processes are well established (Kear et al. 2004, King et al. 2010) and a mixed-potential model has been developed (King et al. 1995a). Briefly, the anodic dissolution reaction proceeds via a two-step process involving an adsorbed $CuCl_{ads}$ intermediate

$$Cu + Cl^- = CuCl_{ads} + e^- \quad (3\text{-}8a)$$

$$CuCl_{ads} + Cl^- = CuCl_2^- \quad (3\text{-}8b)$$

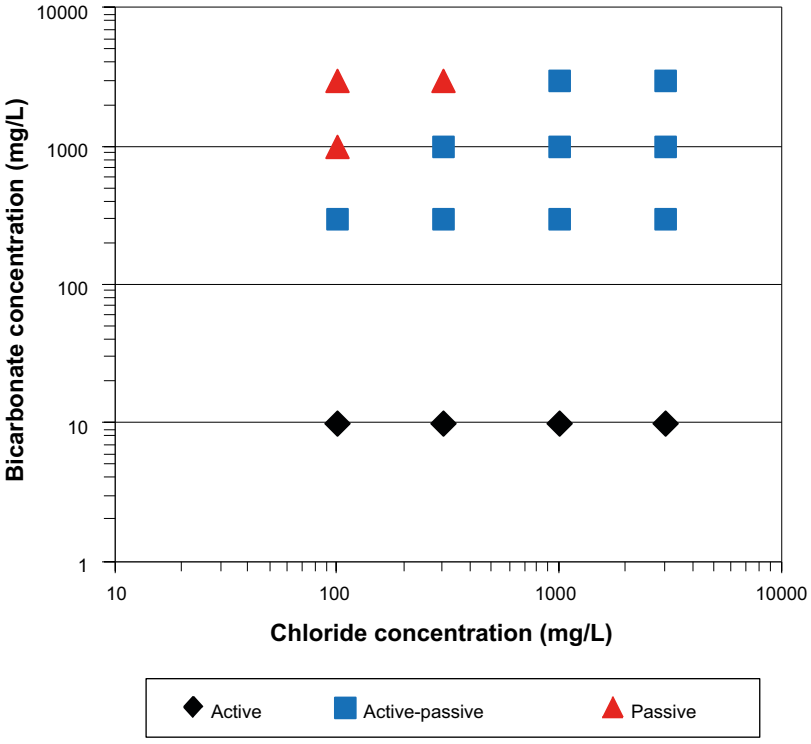

Figure 3-11. *Regions of active, passive, or active-passive behaviour for copper at 30°C and neutral pH as a function of chloride and bicarbonate concentration based on the voltammetric response (Imai et al. 1996).*

The cathodic reaction involves the overall 4-electron reduction of O_2 to OH^-

$$O_2 + 2H_2O + 4e^- \rightarrow 4OH^- \quad (3\text{-}9)$$

although intermediate peroxide species are stable and can be detected under some circumstances (King et al. 1995b, c). Kinetic expressions for these two reactions have been combined to develop a mixed-potential model to predict E_{CORR}, with the model predictions validated over a range of three orders of magnitude variation in dissolved $[O_2]$, one order of magnitude variation in $[Cl^-]$, and five orders of magnitude variation in steady-state mass-transfer coefficient (King et al. 1995a).

The presence of SO_4^{2-} introduces the possibility of direct dissolution of copper as Cu^{2+} since, unlike Cl^-, sulphate does not form stable complexes with Cu(I). King and Tang (1998) studied the dissolution behaviour of Cu in Cl^-/SO_4^{2-} mixtures using a rotating split-ring disc electrode with which any stable Cu(I) or Cu(II) intermediates produced by dissolution of the copper disc could be determined. Figure 3-12 shows the overall reaction mechanism considered by King and Tang (1998) involving dissolution via three possible pathways, namely: (i) a soluble $CuCl_2^-$ species, as in Cl^- solution, (ii) a dissolved Cu^{2+} ion, and (iii) a dissolved Cu^+ ion, the latter two species included as possible stable products of the dissolution of copper in SO_4^{2-} solutions. Even in solutions with a $[Cl^-]:[SO_4^{2-}]$ ratio of 1:10 or $[Cl^-]$ as low as 0.02 mol/L, there was little evidence for the formation of stable Cu(II) species at potentials up to −0.025 V_{SCE}. No evidence for surface oxides was found from cathodic stripping voltammetry following potentiostatic tests. Thus, there is no evidence that copper dissolves as anything other than $CuCl_2^-$ in Cl^-/SO_4^{2-}, which implies that the mixed-potential model based on reactions (3-8) and (3-9) should equally apply to the pore solutions present in compacted bentonite. Indeed, the mixed-potential model has been validated against E_{CORR} values measured using a copper-compacted clay electrode with either a 1-mm or 1-cm-thick clay layer adjacent to the copper surface (King et al. 1995a).

The reaction mechanism is quite different for the general corrosion of copper in the presence of sulphide ions. In this case, the anodic reaction involves the formation of a highly insoluble cuprous sulphide Cu_2S via (Chen et al. 2010, Smith et al. 2011)

$$Cu + HS^- = CuHS_{ads} + e^- \quad (3\text{-}10a)$$

$$CuHS_{ads} + Cu \rightarrow Cu_2S + H^+ + e^- \quad \text{rds} \quad (3\text{-}10b)$$

where the latter process is the rate-determining step (rds). The cathodic reaction is the reduction of H_2O

$$H_2O + e^- \rightarrow \tfrac{1}{2}H_2 + OH^- \quad (3\text{-}11)$$

A mixed-potential model involving these reactions has been developed and has been validated against the results of experimental measurements with a copper-compacted clay electrode (King et al. 2011a, b).

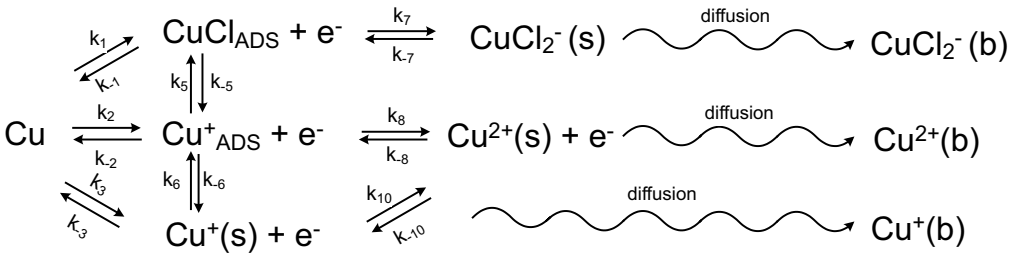

Figure 3-12. *Overall reaction scheme for the dissolution of copper in chloride/sulphate mixtures considered by King and Tang (1998).*

4 Analysis of the localised corrosion behaviour of copper canisters

4.1 Prerequisites for a probabilistic assessment of pitting

Figure 1-1 shows the overall approach used here to address the SSM request for a probabilistic analysis of the pitting of copper canisters. The first steps are to define the canister-surface environment (and how it evolves over time) (Chapter 2) and to review literature data on the pitting of copper (Section 3.2). The crucial next step is to determine whether, under the expected environmental conditions at the canister surface, the canister will be in a passive state and subject to pitting corrosion.

4.1.1 Oxic and early anoxic period

As discussed in Chapter 3, whether the canister surface is passive and susceptible to pitting is a complex function of the pH, temperature, and the concentrations of HCO_3^-, Cl^-, and SO_4^{2-}. Based on the pore-water modelling studies summarized in Table 2-1, the canister surface will be contacted by a near-neutral (pH 7.0–7.9), chloride-rich solution containing approximately 0.001 mol/L HCO_3^- and 0.01–0.02 mol/L SO_4^{2-}. The Cl^- concentration is predicted to increase with time from 0.04 mol/L initially to 0.15 mol/L following equilibration with the surrounding ground water. Whilst the [SO_4^{2-}] and [HCO_3^-] and pH are constrained by the solubility of calcium sulphate (anhydrite at T > 40°C and gypsum at lower temperatures) and by the presence of calcite impurities in the bentonite, respectively, the [Cl^-] is determined primarily by the rate of equilibration of the pore and ground waters.

The conditions under which copper dissolves actively were summarized in Section 3.3. Based on the evidence presented there, it appears that the canister surface will dissolve actively for the following reasons:

1. The pore-water Cl^- concentration exceeds the threshold of 0.034 mol/L for active dissolution defined by Yabuki and Murakami (2007). Although the pore-water [SO_4^{2-}] does not exceed the threshold concentration for active dissolution, for mixed Cl^-/SO_4^{2-} solutions it is reasonable to assume that the surface will be active if either anion is present at a concentration higher than the threshold value.
2. The initial pore-water [Cl^-] (0.04 mol/L, 1,420 mg/L) and [HCO_3^-] (0.001–0.002 mol/L, 60–120 mg/L) are within the "active" zone defined by Imai et al. (1996) (Figure 3-11).
3. The pore-water [HCO_3^-] is below the value of 8,500 mg/L reported by Sridhar and Cragnolino (1993) to induce pitting and similar to the value of 85 mg/L at which only general corrosion was observed. The test solution of 85 mg/L (0.0014 mol/L) HCO_3^-, 1,000 mg/L (0.028 mol/L) Cl^-, and 1,000 mg/L (0.01 mol/L) SO_4^{2-} (Sridhar and Cragnolino 1993) is similar to the pore-water composition in Table 2-1. In this solution, Sridhar and Cragnolino (1993) only observed general corrosion without pitting at both 30°C and 95°C, even though the solution pH of 8.0–9.7 (higher than the predicted pore water pH of 7.0–7.9) would be more likely to induce passivity.
4. In mixed Cl^-/SO_4^{2-} solutions similar to those of the predicted pore-water composition, King and Tang (1998) observed only active dissolution of copper as the dissolved $CuCl_2^-$ species and found no evidence for film formation.

It is also interesting to note that none of the reported E_b values in Section 3.2 were determined in conditions similar to those expected at the canister surface. In both Cl^- and SO_4^{2-} solutions, there is a clear tendency to an increasing number of E_b measurements with increasing pH and increasing [HCO_3^-], both conditions promoting passivation of the surface. There are relatively few reports of E_b values at pH 7–8, the range corresponding to the pH of bentonite pore water. In Cl^- solutions (Figure 3-2), the only E_b measurements at pH < 8 are those of Gad Allah et al. (1991) at pH 7.26 for [Cl^-] of 0.05–0.5 mol/L. For a [Cl^-] of 0.1 mol/L, corresponding to the maximum pore-water concentration during the aerobic phase (Table 2-1), the measured E_b value is 0.40 V_{SCE}. The only data reported for pH 8 are those of Imai et al. (1996) in solutions containing 0.005–0.049 mol/L HCO_3^-, i.e., a factor of 5–50 times higher than in the bentonite pore water. (Note: the pH value of 8

is an assumed value by the present authors because Imai et al. (1996) did not define the pH of the test solutions, which may have been > pH 8). Similarly, in SO_4^{2-} solutions (Figure 3-3), the only E_b measurements at pH ≤ 8 are those of Imai et al. (1996) in bicarbonate-containing solutions at an assumed pH of 8.

Cong et al. (2009a, b) do report pitting at pH 7–8 and have provided expressions for estimating values of E_b and E_{rp} based on the pH, $[HCO_3^-]$, $[Cl^-]$, and $[SO_4^{2-}]$ (Equations (3-3) to (3-7)). Table 4-1 summarises the calculated pitting and re-passivation potentials (the latter based on both the SO_4^{2-} and Cl^- concentrations) for the canister surface pore-water compositions from Chapter 2. The predicted E_b and E_{rp} values are shown in relation to the stability fields for Cu, Cu_2O, and $Cu(OH)_2$ in Figure 4-1. It is apparent from both the table and figure that the expressions developed by Cong et al. (2009a, b) do not apply in the case of the bentonite pore-water composition since the predicted re-passivation potentials are more positive than the predicted breakdown potential, a situation that makes no physical sense. Furthermore, the predicted potentials lie below the $Cu_2O/Cu(OH)_2$ equilibrium line, which Cong et al. (2009a, b) considered to represent a threshold for pitting (Figure 3-9).

There are two possible explanations why the expressions of Cong et al. (2009a, b) are not applicable in the case of bentonite pore water. First, as Cong et al. (2009a, b) themselves acknowledged, the expressions may not be valid outside of the range of experimental conditions on which the fitted equations were based. However, Cong et al. (2009a, b) used a wide range of solution compositions for the HCO_3^-/SO_4^{2-} and HCO_3^-/Cl^- systems at pH 8.3 and 9.5 (0.00068–0.01 mol/L HCO_3^- and approximately 10^{-4} mol/L to 0.5 mol/L SO_4^{2-} and Cl^-) and a wide range of pH (pH 5–11) for one of the synthetic potable waters studied. The second possible explanation is that the fitted expressions may simply no longer be valid because the copper surface is not subject to pitting in the bentonite pore waters, but instead dissolves actively. Thus, the combination of low $[HCO_3^-]$, low pH, and relatively high $[Cl^-]$ and $[SO_4^{2-}]$ in the bentonite pore water promote active dissolution rather than passivity.

Table 4-1. Predicted pitting and re-passivation potentials based on the pore-water compositions in Table 2-1 and the expressions for E_b and E_{rp} of Cong et al. (2009a, b).

(a) 10-year bentonite saturation, high advective flow in fracture

Time (years)	Temp. (°C)	pH	$[HCO_3^-]$ (mol/kg)	$[Cl^-]$ (mol/kg)	$[SO_4^{2-}]$ (mol/kg)	E_b* (V_{SCE})	E_{rp}** (V_{SCE})	E_{rp}*** (V_{SCE})
0	46	7.86	0.0011	0.040	0.0146	–0.025	–0.078	0.005
1	71	7.36	0.0011	0.040	0.0097	–0.078	–0.070	0.003
10	80	7.17	0.0014	0.072	0.0084	–0.104	–0.058	–0.014
100	63	7.12	0.0016	0.094	0.0115	–0.112	–0.061	–0.021
1,000	41	6.96	0.0021	0.147	0.0156	–0.132	–0.060	–0.034
10,000	20	7.07	0.0022	0.154	0.0149	–0.118	–0.057	–0.035

* Based on the combined expression for Cl^- and SO_4^{2-}, Equation (3-7).
** Based on the re-passivation potential for SO_4^{2-} environments, Equation (3-4).
*** Based on the re-passivation potential for Cl^- environments, Equation (3-6).

(b) 10-year bentonite saturation, low advective flow in fracture

Time (years)	Temp. (°C)	pH	$[HCO_3^-]$ (mol/kg)	$[Cl^-]$ (mol/kg)	$[SO_4^{2-}]$ (mol/kg)	E_b* (V_{SCE})	E_{rp}** (V_{SCE})	E_{rp}*** (V_{SCE})
0	46	7.86	0.0011	0.040	0.0146	–0.025	–0.078	0.005
1	71	7.36	0.0011	0.040	0.0097	–0.077	–0.069	0.003
10	80	7.12	0.0013	0.072	0.0084	–0.112	–0.059	–0.014
100	63	7.05	0.0014	0.082	0.0115	–0.123	–0.065	–0.017
1,000	41	7.12	0.0015	0.084	0.0156	–0.117	–0.072	–0.018
10,000	20	7.27	0.0016	0.092	0.0149	–0.097	–0.068	–0.020

* Based on the combined expression for Cl− and SO_4^{2-}, Equation (3-7).
** Based on the re-passivation potential for SO_4^{2-} environments, Equation (3-4).
*** Based on the re-passivation potential for Cl^- environments, Equation (3-6).

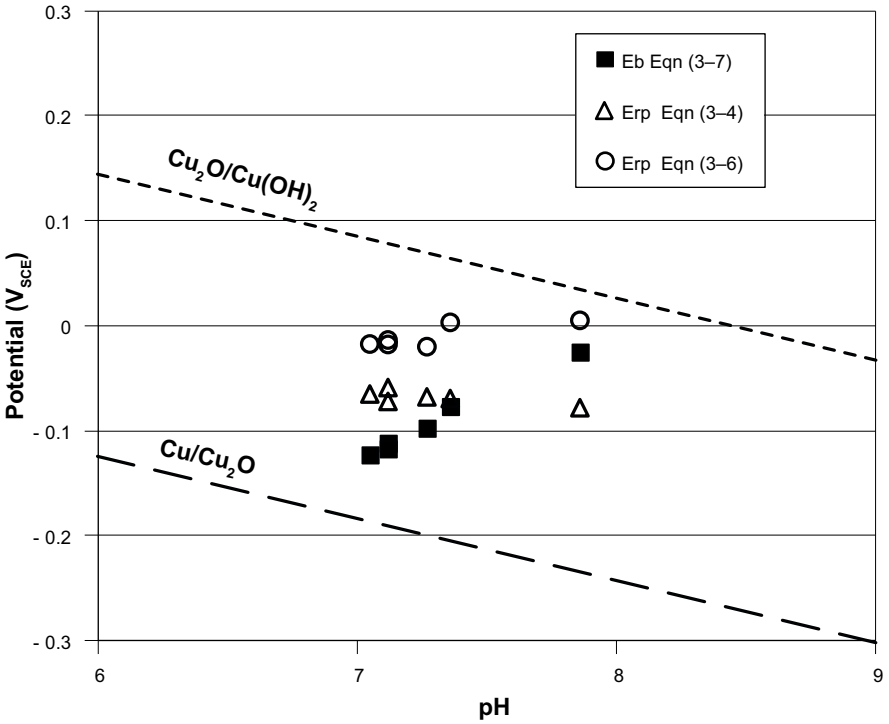

Figure 4-1. *Predicted pitting and re-passivation potentials for the bentonite pore water at the canister surface for the case of 10-year saturation and low advective flow (Table 4-1(b)) based on the relationships between critical potential and solution composition of Cong et al. (2009a, b).*

The conclusion that the canister surface will not be susceptible to pitting corrosion in the bentonite pore water is consistent with the results from large-scale *in situ* tests and from laboratory corrosion experiments performed under simulated repository conditions. As discussed in Section 3.1, and illustrated in Figure 3-1, all of the available evidence suggests that the canister surface will corrode actively, with a certain degree of surface roughening. The profile shown in Figure 3-1 is not consistent with a passive surface that undergoes local breakdown and discrete pit growth.

4.1.2 Long-term anoxic period

A similar conclusion is reached for the nature of the copper surface under anoxic conditions in the presence of sulphide. Chen et al. (2010, 2011a, b, 2012) have shown that the properties of the Cu_2S film that forms on copper exposed to HS^- in chloride solutions depends on the concentrations of Cl^- and HS^-, and the rate of mass transport (Figure 4-2). In bulk solution, at high [HS^-] (of the order of millimolar and higher), compact films are formed characterised by a parabolic growth law. At lower [HS^-], the film is porous (type P1 in Figure 4-2) with linear growth limited by the slow transport of HS^- to the copper surface. Another type of porous film with columnar structure is observed at high [Cl^-] (greater than approximately 5 mol/L), type P2 in Figure 4-2. Slow rates of mass transport, or most likely low HS^- fluxes, also promote the formation of porous films, so that the film formed under repository conditions is expected to be porous. Crucially, Chen and co-workers have not observed any evidence for pitting for any of these three types of surface film during either freely corroding or polarization studies.

This tendency towards more-compact and potentially passivating Cu_2S films on copper at higher [HS^-] reported by Chen and co-workers is consistent with the reports of pitting by Gennero de Chialvo and Arvia (1985) and Vasquez Moll et al. (1985). These latter authors worked at a minimum [HS^-] of 0.001 mol/L at which, based on the evidence in Figure 4-2, compact films would be expected, which might then be susceptible to film breakdown at more-positive potentials.

As in the case of sulphide-free environments, therefore, it is concluded that the canister surface will not be passivated by the presence of realistic pore-water [HS^-] and will not be susceptible to pitting.

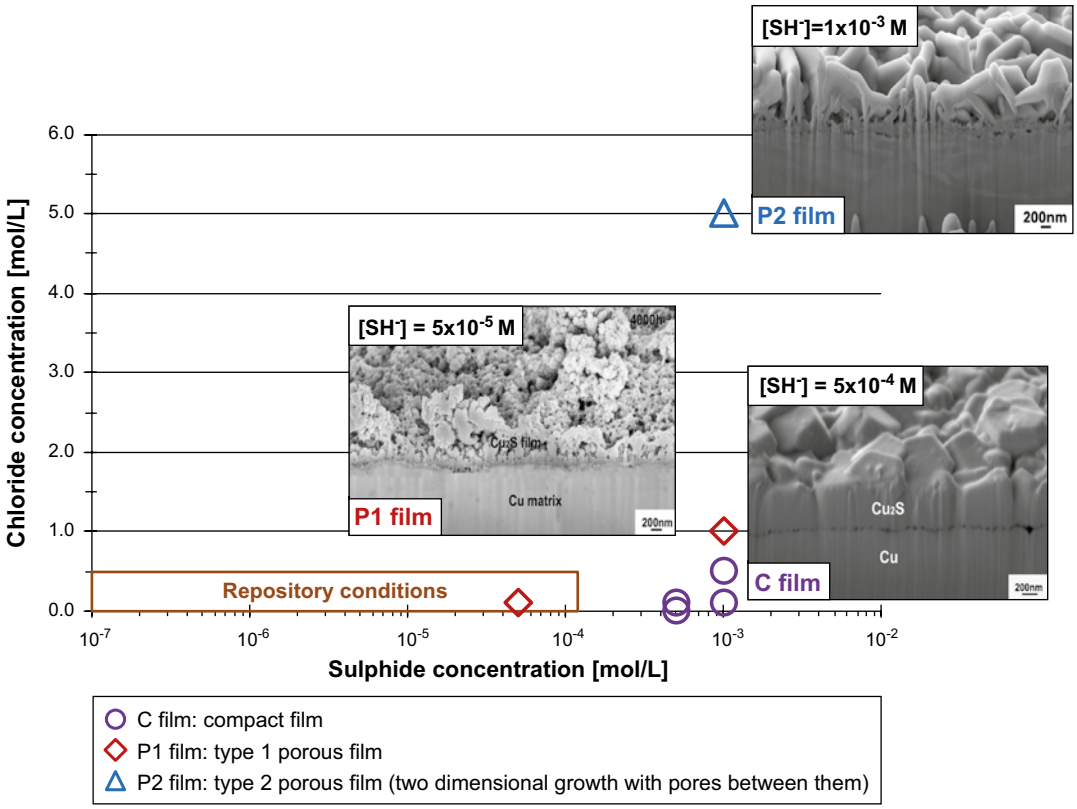

Figure 4-2. *Relationship between the concentrations of chloride and sulphide ions and the properties of the Cu_2S films formed on copper under naturally corroding conditions. The area marked "Repository conditions" indicates the concentrations conceivable at the Forsmark site (SKB 2010b).*

4.1.3 Conclusion for probabilistic assessment

In summary, we have attempted to address the SSM request for a probabilistic assessment of the pitting of copper canisters following the approach outlined in Figure 1-1. It has been concluded, however, that the canister surface will undergo active dissolution in contact with bentonite pore waters and is not susceptible to pitting. This conclusion is consistent with the absence of pitting and the observation of surface roughening of copper exposed to repository environments and the lack of literature pitting data for bentonite pore-water compositions.

4.2 Effect of surface deposits and salt enrichment

The SSM request for additional information on the localised corrosion of copper (SSM 2012) also questioned the possible role of salt deposits on pitting. We are unaware of any studies that have considered the effects of surface salts on the pitting of copper (or of any other material). The formation of surface deposits has been implicated in the surface roughening of copper (which, at one time, was referred to as "under-deposit" corrosion), for which a tentative mechanism has been proposed (King et al. 2010).

Cong and Scully (2013) and Cong et al. (2007) have considered the effects of $Al(OH)_3$ on the pitting of copper in potable waters. The layer of $Al(OH)_3$ was considered to both physically occlude the surface and, as a result of its anion-exchange properties, lower the pH at the copper surface. As a result, the pitting potential was reduced compared to the value in bulk solution, which would increase the probability of pitting (on the assumption that there was no corresponding shift in E_{CORR} in the presence of the $Al(OH)_3$ membrane).

There is no evidence that the presence of compacted bentonite will increase the susceptibility of copper to pitting. All of the evidence from large-scale *in situ* studies and laboratory experiments in which copper has been exposed to compacted bentonite indicates that the surface undergoes general corrosion with a certain degree of roughening but not pitting corrosion (Section 3.1). Unlike $Al(OH)_3$, montmorillonite is a cation-exchanger and the presence of calcite impurities in naturally occurring bentonite will buffer the pore-water pH. Although the presence of the compacted bentonite may occlude parts of the surface, which may in part explain the observation of surface roughening of copper surfaces, there is no evidence that this leads to permanent spatial separation of anodic and cathodic processes.

The bentonite pore-water compositions that have been used in the analyses described above were derived taking into account the various processes that will occur in the buffer material under repository conditions, including ion exchange, pH buffering, and the precipitation and dissolution of salts (Sena et al. 2010a). It is believed, therefore, that the bentonite pore-water compositions used in the analyses properly represent the net effect of the clay properties and of the thermal gradient on the development of the pore water and on the consequent corrosion behaviour under repository conditions. Even if more-saline conditions are formed at the canister surface, as has been found for heated surfaces in contact with bentonite in some cases (Section 2.1), the enrichment of Cl^- and/or SO_4^{2-} will tend to promote active dissolution rather than passivity and possible localised corrosion (Section 3.3). This conclusion is consistent with the absence of pits on heated copper surfaces exposed to compacted bentonite in the LOT experiment (Karnland et al. 2000).

In conclusion, it is not believed that surface deposits, whether in the form of cation-exchanging bentonite, precipitated corrosion products, or accumulated salt deposits, will promote the pitting of the canisters.

4.3 Effect of radiolysis

There are two possible effects of γ-radiolysis products on the pitting of copper, namely (i) the effect of irradiation on E_b (and E_{rp}) and (ii) the effect on E_{CORR}. As discussed in Section 3.2.3, there are no measurements of E_b in the presence of radiation, although there is some indication from the data of Imai et al. (1996) that the pitting potential may shift to more-positive values with increasing redox potential (Figure 3-8). Although Glass et al. (1985) observed a 100 mV positive shift in E_{CORR} in dilute synthetic ground water at 30°C at an absorbed dose rate of 3×10^4 Gy/h, King and Litke (1987) observed no effect on E_{CORR} in a saline synthetic ground water at 150°C with the repeated insertion and withdrawal of a gamma source providing an absorbed dose rate of 27 Gy/h. Since the maximum absorbed dose rate at the surface of a copper canister is <1 Gy/h (SKB 2010a), no effect of irradiation on the E_{CORR} would be expected.

There is no evidence, therefore, that the probability of pitting of copper, as measured by the difference between E_b and E_{CORR}, is higher for a gamma dose rate of the magnitude of that expected for a copper canister.

4.4 Effect of temperature

Under environmental conditions for which copper is susceptible to pitting, the available evidence suggests that the probability of pitting decreases with increasing temperature. Figure 3-7 summarises the dependence of E_b on temperature in Cl^- and Cl^-/HCO_3^- environments based on data from the literature. At temperatures >15°C, E_b increases with increasing temperature. The E_{CORR} of copper decreases with increasing temperature, in part because of the negative temperature dependence of the standard potential for the anodic and cathodic reactions (King et al. 2008). The net effect, therefore, is that the difference between E_{CORR} and E_b increases significantly with increasing temperature and the probability of pitting decreases.

This conclusion is consistent with the observations of Sridhar and Cragnolino (1993) who, for those conditions under which pitting occurred at 30°C, observed general corrosion at a temperature of 95°C.

5 Summary and conclusions

In response to a request from SSM for additional information, an analysis has been performed of the expected localised corrosion behaviour of copper canisters. The analysis is based on a critical review of literature information on the pitting of copper and an assessment of the environmental conditions to which the canister will be exposed.

The analysis involved a comparison of the environmental conditions at the canister surface with those known to induce the pitting of copper. Based on this comparison, it has been concluded that copper canisters will not be susceptible to pitting corrosion but will instead undergo general corrosion with a certain degree of surface roughening. This conclusion is consistent with the observations from full-scale in situ tests at Äspö and with the results of laboratory experiments in simulated repository environments.

The canister is expected to dissolve actively in the absence of passivation during both he initial warm aerobic phase and during the long-term anoxic period dominated by the presence of sulphide. The salinity of the bentonite pore water is too high, and the pore-water bicarbonate concentration and pH are too low, to induce passivation of the copper surface. In the presence of sulphide, the surface cuprous sulphide film will be porous rather than passive for the sulphide concentrations expected in the repository. Because of the absence of passivity, the surface will corrode generally and will not be subject to localised film breakdown and pitting.

References

SKB's (Svensk Kärnbränslehantering AB) publications can be found at www.skb.se/publications.

Arcos D, Bruno J, Benbow S, Takase H, 2000. Behaviour of bentonite accessory minerals during the thermal stage. SKB TR-00-06, Svensk Kärnbränslehantering AB.

Bruno J, Arcos D, Duro L, 1999. Processes and features affecting the near field hydrochemistry. Groundwater–bentonite interaction. SKB TR-99-29, Svensk Kärnbränslehantering AB.

Chen J, Qin Z, Shoesmith D W, 2010. Kinetics of corrosion film growth on copper in neutral chloride solutions containing small concentrations of sulfide. Journal of The Electrochemical Society 157, C338–C345.

Chen J, Qin Z, Shoesmith D W, 2011a. Rate controlling reactions for copper corrosion in anaerobic aqueous sulphide solutions. Corrosion Engineering, Science and Technology 46, 138–141.

Chen J, Qin Z, Shoesmith D W, 2011b. Long-term corrosion of copper in a dilute anaerobic sulfide solution. Electrochimica Acta 56, 7854–7861.

Chen J, Qin Z, Shoesmith D W, 2012. Copper corrosion in aqueous sulfide solutions under nuclear waste repository conditions. In scientific basis for nuclear waste management XXXV: symposium held in Buenos Aires, Argentina, 2–7 October 2011. Warrendale, PA: Materials Research Society. (Materials Research Society Symposium Proceedings 1475), 465–470.

Christy A G, Lowe A, Otieno-Alego V, Stoll M, Webster R D, 2004. Voltammetric and Raman microscopic studies on artificial copper pits grown in simulated potable water. Journal of Applied Electrochemistry 34, 225–233.

Cong H, 2009. Understanding the interplay between water chemistry and electrochemical properties of copper. PhD thesis. University of Virginia.

Cong H, Scully J R, 2013. Effects of aluminum solids on the under deposit corrosion of copper in synthetic potable water: the arguments for and against a semi-permeable membrane. Journal of The Electrochemical Society 160, C403–C413.

Cong H, Budiansky N D, Michels H T, Scully J, 2007. Use of coupled electrode arrays to elucidate copper pitting as a function of potable water chemistry. ECS Transactions 3, 531–544.

Cong H, Michels H T, Scully J R, 2009a. Passivity and pit stability behavior of copper as a function of selected water chemistry variables. Journal of The Electrochemical Society 156, C16–C27.

Cong H, Michels H T, Scully J R, 2009b. Passivity and pit stability behavior of copper as a function of selected water chemistry variables. In Weidner J, Fujimoto S, Frankel G S, Haruna T (eds). Critical factors in localized corrosion 6, in honor of professor Shibata. Pennington, NJ: The Electrochemical Society. (ECS Transactions 16), 141–164.

Cuevas J, Villar M V, Fernandez A M, Gomez P, Martin P L, 1997. Pore waters extracted from compacted bentonite subjected to simultaneous heating and hydration. Applied Geochemistry 12, 473–481.

Curti E, Wersin P, 2002. Assessment of porewater chemistry in the bentonite backfill for the Swiss SF/HLW repository. Nagra NTB 02-09, Nagra, Switzerland.

de Chialvo M R G, Salvarezza R C, Vasquez Moll D, Arvia A J, 1985. Kinetics of passivation and pitting corrosion of polycrystalline copper in borate buffer solutions containing sodium chloride. Electrochimica Acta 30, 1501–1511.

Dixon D A, Chandler N A, Wan A W-L, Stroes-Gascoyne S, Graham J, Oscarson D W, 1998. Pre- and post-test properties of the buffer, backfill, sand and rock components of the buffer/container experiment. AECL-11786, COG-97-287-I, Atomic Energy of Canada Limited.

Drogowska M, Brossard L, Ménard H, 1992. Copper dissolution in $NaHCO_3$ and $NaHCO_3$ + NaCl aqueous solutions at pH 8. Journal of The Electrochemical Society 139, 39–47.

Duthil J-P, Mankowski G, Giusti G, 1996. The synergistic effect of chloride and sulphate on pitting corrosion of copper. Corrosion Science 38, 1839–1849.

Edwards M, Rehring J, Meyer T, 1994. Inorganic anions and copper pitting. Corrosion 50, 366–372.

Figueroa M G, Salvarezza R C, Arvia A J, 1986. The influence of temperature on the pitting corrosion of copper. Electrochimica Acta 31, 665–669.

Gad Allah A G, Abou-Romia M M, Badawy W A, Rehan H H, 1991. Effect of halide ions on passivation and pitting corrosion of copper in alkaline solutions. Werkstoffe und Korrosion 42, 584–591.

Gennero de Chialvo M R, Arvia A J, 1985. The electrochemical behaviour of copper in alkaline solutions containing sodium sulphide. Journal of Applied Electrochemistry 15, 685–696.

Glass R S, Van Konynenburg R A, Overturf G E, 1985. Corrosion processes of austenitic stainless steels and copper-based materials in gamma-irradiated aqueous environments. Report UCRL-92941, Lawrence Livermore National Laboratory.

Gonzalez S, Laz M M, Souto R M, Salvarezza R C, Arvia A J, 1993. Synergistic effects in the inhibition of copper corrosion. Corrosion 49, 450–456.

Imai H, Fukuda T, Akashi M, 1996. Effects of anionic species on the polarization behavior of copper for waste package material in artificial ground water. In Murphy W A, Dieter A K (eds). Scientific basis for nuclear waste management XIX: symposium held in Boston, Massachusetts, USA, 27 November – 1 December 1995. Pittsburgh, PA: Materials Research Society. (Materials Research Society Symposium Proceedings 412), 589–596.

Karnland O, Sandén T, Johannesson L-E, Eriksen T E, Jansson M, Wold S, Pedersen K, Motamedi M, Rosborg B, 2000. Long term test of buffer material. Final report on the pilot parcels. SKB TR-00-22, Svensk Kärnbränslehantering AB.

Karnland O, Olsson S, Dueck A, Birgersson M, Nilsson U, Hernan-Hakansson T, Pedersen K, Nilsson S, Eriksen T-E, Rosborg B, 2009. Long term test of buffer material at the Äspö Hard Rock Laboratory, LOT project. Final report on the A2 test parcel. SKB TR-09-29, Svensk Kärnbränslehantering AB.

Kear G, Barker B D, Walsh F C, 2004. Electrochemical corrosion of unalloyed copper in chloride media – a critical review. Corrosion Science 46, 109–135.

King F, 2002. Corrosion of copper in alkaline chloride environments. SKB TR-02-25, Svensk Kärnbränslehantering AB.

King F, Kolář M, 2006. Simulation of the consumption of oxygen in long-term in situ experiments and in the third case study repository using the copper corrosion model CCM-UC.1.1. Report 06819-REP 0130010084 R00, Ontario Power Generation, Nuclear Waste Management Division, Canada.

King F, Litke C D, 1987. The corrosion of copper in synthetic groundwater at 150 degrees C. Part I: the results of short term electrochemical tests. Technical Record TR-428, Atomic Energy of Canada Limited.

King F, Tang Y, 1998. The anodic dissolution of copper in chloride-sulphate groundwaters. Report 06819-REP-01200-0058 R00, Ontario Hydro, Nuclear Waste Management Division, Canada.

King F, Litke C D, Quinn M J, LeNeveu D M, 1995a. The measurement and prediction of the corrosion potential of copper in chloride solutions as a function of oxygen concentration and mass transfer coefficient. Corrosion Science 37, 833–851.

King F, Quinn M J, Litke C D, 1995b. Oxygen reduction on copper in neutral NaCl solution. Journal of Electroanalytical Chemistry 385, 45–55.

King F, Litke C D, Tang Y, 1995c. Effect of interfacial pH on the reduction of oxygen on copper in neutral $NaClO_4$ solution. Journal of Electroanalytical Chemistry 384, 105–113.

King F, Kolář M, Maak P, 2008. Reactive-transport model for the prediction of the uniform corrosion behaviour of copper used fuel containers. Journal of Nuclear Materials 379, 133–141.

King F, Lilja C, Pedersen K, Pitkänen P, Vähänen M, 2010. An update of the state-of-the-art report on the corrosion of copper under expected conditions in a deep geologic repository. SKB TR-10-67, Svensk Kärnbränslehantering AB.

King F, Kolář M, Vähänen M, 2011a. Reactive-transport modelling of the sulphide-assisted corrosion of copper nuclear waste containers. In Féron D, Kursten B, Druyts F (eds). Sulphur-assisted corrosion in nuclear disposal systems. Leeds, UK: Maney Publishing. (European Federation of Corrosion Publications 59), 152–164.

King F, Kolář M, Vähänen M, Lilja C, 2011b. Modelling long term corrosion behaviour of copper canisters in a KBS-3 repository. Corrosion Engineering Science and Technology 46, 217–222.

Lemire R J, Garisto F, 1989. The solubility of U, Np, Pu, Th and Tc in a geological disposal vault for used nuclear fuel. AE Report CL-10009, Atomic Energy of Canada Limited.

Litke C D, Ryan S R, King F, 1992. A mechanistic study of the uniform corrosion of copper in compacted clay-sand soil. Report AECL-10397, COG-91-304, Atomic Energy of Canada Limited.

Luukkonen A, 2004. Modelling approach for geochemical changes in the prototype repository engineered barrier system. Posiva Working Report 2004-31, Posiva Oy, Finland.

Mankowski G, Duthil J P, Giusti A, 1997. The pit morphology on copper in chloride- and sulphate-containing solutions. Corrosion Science 39, 27–42.

Mattsson E, Frederiksson A-M, 1968. Pitting corrosion in copper tubes – cause of corrosion and counter-measures. British Corrosion Journal 3, 246–257.

Milošev I, Metikoš-Huković M, Drogowska M, Ménard H, Brossard L, 1992. Breakdown of passive film on copper in bicarbonate solutions containing sulphate ions. Journal of The Electrochemical Society 139, 2409–2418.

Muurinen A, 2006. Chemical conditions in the A2 parcel of the long-term test of buffer material in Äspö (LOT). Posiva Working Report 2006-83, Posiva Oy, Finland.

Muurinen A, Carlsson T, 2010. Experiences pf pH and Eh measurements in compacted MX-80 bentonite. Applied Clay Science 47, 23–27.

Muurinen A, Lehikoinen J, 1999. Porewater chemistry in compacted bentonite. Engineering Geology 54, 207–214.

Nagra, 2002. Project Opalinus Clay. Safety report. Nagra Technical Report 02-05, Nagra, Switzerland.

Nishikata A, Itagaki M, Tsuru T, Haruyama S, 1990. Passivation and its stability on copper in alkaline solutions containing carbonate and chloride ions. Corrosion Science 31, 287–292.

Olsson S, Jensen V, Johannesson L-E, Hansen E, Karnland O, Kumpulainen S, Kiviranta L, Svensson D, Hansen S, 2013. Prototype Repository. Hydro-mechanical, chemical and mineralogical characterization of the buffer and tunnel backfill material from the outer section of the Prototype Repository. SKB TR-13-21, Svensk Kärnbränslehantering AB.

Posnjak E, 1938. The system, $CaSO_4$-H_2O. American Journal of Science 235A, 247–272.

Pourbaix M, 1969. Recent applications of electrode potential measurements in the thermodynamics and kinetics of corrosion of metals. Corrosion 25, 267–281.

Puigdomenech I, Ambrosi J-P, Eisenlohr L, Lartigue J-E, Banwart S A, Bateman K, Milodowski A E, West J M, Griffault L, Gustafsson E, Hama K, Yoshida H, Kotelnikova S, Pedersen K, Michaud V, Trotignon L, Rivas Perez J, Tullborg E-L, 2001. O_2 depletion in granitic media. The REX project. SKB TR-01-05, Svensk Kärnbränslehantering AB.

Qafsaoui W, Mankowski G, Dabosi F, 1993. The pitting corrosion of pure and low alloyed copper in chloride-containing borate buffered solutions. Corrosion Science 34, 17–25.

Rosborg R, 2013. Post-test examination of a copper electrode from the deposition hole 5 in the Prototype Repository. SKB R-13-14, Svensk Kärnbränslehantering AB.

Rosborg B, Werme L, 2008. The Swedish nuclear waste program and the long-term corrosion behaviour of copper. Journal of Nuclear Materials 379, 142–153.

Sena C, Salas J, Arcos D, 2010a. Aspects of geochemical evolution of the SKB near field in the frame of SR-Site. SKB TR-10-59, Svensk Kärnbränslehantering AB.

Sena C, Salas J, Arcos D, 2010b. Thermo-hydro-geochemical modelling of the bentonite buffer. LOT A2 experiment. SKB TR-10-65, Svensk Kärnbränslehantering AB.

Scully J R, Hicks T W, 2012. Initial review phase for SKB's safety assessment SR-Site: corrosion of copper. Technical Note 2012:21, Strålsäkerhetsmyndigheten (Swedish Radiation Safety Authority).

SKB, 2010a. Fuel and canister process report for the safety assessment SR-Site. SKB TR-10-46, Svensk Kärnbränslehantering AB.

SKB, 2010b. Comparative analysis of safety related site characteristics. SKB TR-10-54, Svensk Kärnbränslehantering AB.

SKB, 2011. Long-term safety for the final repository for spent nuclear fuel at Forsmark. Main Report of the SR-Site project. SKB TR-11-01, Svensk Kärnbränslehantering AB.

Skrypnikova E A, Kaluzhina S, Bocharova I, 2008. Benzotriazole influence on copper pitting corrosion in hydrocarbonate-chloride solutions under different temperature. ECS Transactions 6, 73–78.

Smith J M, Qin Z, King F, Shoesmith D W, 2011. The influence of chloride on the corrosion of copper in aqueous sulfide solutions. In Féron D, Kursten B, Druyts F (eds). Sulphur-assisted corrosion in nuclear disposal systems. Leeds, UK: Maney Publishing. (European Federation of Corrosion Publications 59), 109–123.

Souto R M, González S, Salvarezza R C, Arvia A J, 1994. Kinetics of copper passivation and pitting corrosion in Na_2SO_4 containing dilute NaOH aqueous solution. Electrochim. Acta 39, 2619–2628.

Sridhar N, Cragnolino G A, 1993. Effects of environment on localized corrosion of copper-based, high-level waste container materials. Corrosion 49, 967–976.

SSM, 2012. Begäran om komplettering av ansökan om slutförvaring av använt kärnbränsle och kärnavfall – degraderingsprocesser för kapseln. Dnr SSM2011-2426-57, Strålsäkerhetsmyndigheten (Swedish Radiation Safety Authority). (In Swedish.)

Svensson D, Dueck A, Nilsson U, Olsson S, Sandén T, Lydmark S, Jägerwall S, Pedersen K, Hansen S, 2011. Alternative buffer material. Status of the ongoing laboratory investigations of reference materials and test package 1. SKB TR-11-06, Svensk Kärnbränslehantering AB.

Taxén C, Lundholm M, Persson D, Jakobsson D, Sedlakova M, Randelius M, Karlsson O, Rydgren P, 2012. Analyser av koppar från prototypkapsel 5 och 6. SKB P-12-22, Svensk Kärnbränslehantering AB. (In Swedish.)

Thomas J G N, Tiller A K, 1972a. Formation and breakdown of surface films on copper in sodium hydrogen carbonate and sodium chloride solutions. I. Effects of anion concentrations. British Corrosion Journal 7, 256–262.

Thomas J G N, Tiller A K, 1972b. Formation and breakdown of surface films on copper in sodium hydrogen carbonate and sodium chloride solutions. II. Effects of temperature and pH. British Corrosion Journal 7, 263–267.

Vasquez Moll D, de Chialvo M R G, Salvarezza R C, Arvia A J, 1985. Corrosion and passivity of copper in solutions containing sodium sulphide. Analysis of potentiostatic current transients. Electrochim. Acta 30, 1011–1016.

Wersin P, Spahiu K, Bruno J, 1994. Kinetic modelling of bentonite-canister interaction. Long-term predictions of copper canister corrosion under oxic and anoxic conditions. SKB TR 94-25, Svensk Kärnbränslehantering AB.

Xie M, Bauer S, Kolditz O, Nowak T, Shao H, 2006. Numerical simulation of reactive processes in an experiment with partially saturated bentonite. Journal of Contaminant Hydrology 83, 122–147.

Yabuki A, Murakami M, 2007. Critical ion concentration for pitting and general corrosion of copper. Corrosion 63, 249–257.